AD NUMBER
AD843108
LIMITATION CHANGES

TO:

Approved for public release; distribution is unlimited.

FROM:

Distribution authorized to U.S. Gov't. agencies and their contractors; Critical Technology; SEP 1968. Other requests shall be referred to Air Force Technical Application Center, Washington, DC 20333. This document contains export-controlled technical data.

AUTHORITY

usaf ltr, 25 jan 1972

AD843108

ANALYSIS OF SUMMER LONG-PERIOD NOISE

Special Scientific Report No. 24
LARGE-ARRAY SIGNAL AND NOISE ANALYSIS

Prepared by
Aftab Alam

Frank H. Binder, Program Manager
Telephone: 1-214-238-3491

TEXAS INSTRUMENTS INCORPORATED
Science Services Division
P.O. Box 5621
Dallas, Texas 75222

Contract No. AF 33(657)-16678

Prepared for
AIR FORCE TECHNICAL APPLICATIONS CENTER
Washington, D.C. 20333

Sponsored by
ADVANCED RESEARCH PROJECTS AGENCY
ARPA Order No. 599
AFTAC Project No. VT/6707

NOV 18 1968

A

27 September 1968

STATEMENT #2 UNCLASSIFIED

science services division

63

ANALYSIS OF SUMMER LONG-PERIOD NOISE

Special Scientific Report No. 24
LARGE-ARRAY SIGNAL AND NOISE ANALYSIS

Prepared by
Aftab Alam

Frank H. Binder, Program Manager
Telephone: 1-214-238-3491

TEXAS INSTRUMENTS INCORPORATED
Science Services Division
P.O. Box 5621
Dallas, Texas 75222

Contract No. AF 33(657)-16678

Prepared for
AIR FORCE TECHNICAL APPLICATIONS CENTER
Washington, D.C. 20333

Sponsored by
ADVANCED RESEARCH PROJECTS AGENCY
ARPA Order No. 599
AFTAC Project No. VT/6707

27 September 1968

BLANK PAGE

TABLE OF CONTENTS

TABLE

ILLUSTRATIONS

ILLUSTRATIONS (CONTD)

ILLUSTRATIONS (CONTD)

SECTION I

INTRODUCTION AND PRINCIPAL RESULTS

This report presents results of an analysis of the long-period (LP) noise recorded at the Large-Aperture Seismic Array (LASA) during the summer of 1967. A similar analysis for winter 1966-67 noise was published in Large-Array Signal and Noise Analysis Special Report No. 12.[1]

The LASA long-period system consists of 21 long-period 3-component seismometers located at the center of each subarray at the Montana LASA. A map of the subarray locations and their coordinates (relative to A0) are shown in Figure I-1. Amplitude response of the instrument-amplifier-filter combination used during the data recording is shown in Figure I-2.

In general, the summer noise is similar to the quiet winter noise.[1] Salient features of the summer noise are as follows.

- The noise can be divided into two components: a nonpropagating component below about 0.05 Hz and a propagating component dominating the 0.05- to 0.17-Hz region.

- Fundamental-mode Rayleigh-wave energy seems to dominate the propagating component; however, mantle P-wave energy (0.13 Hz) has also been detected in one case.

- Little coherence has been observed between microbarographic and seismic data; however, this observation is based on the analysis of only five samples, four of which were recorded consecutively.

- Propagating noise shows two regions of high coherence: one between 0.05 and 0.07 Hz and the other between 0.11 and 0.14 Hz. Vertical components can be predicted accurately from the horizontal instruments or from other vertical instruments.

0 10 20 30 40 50 Km

November 1965

SUB-ARRAY A0
46° 41' 19" N
106° 13' 20" W
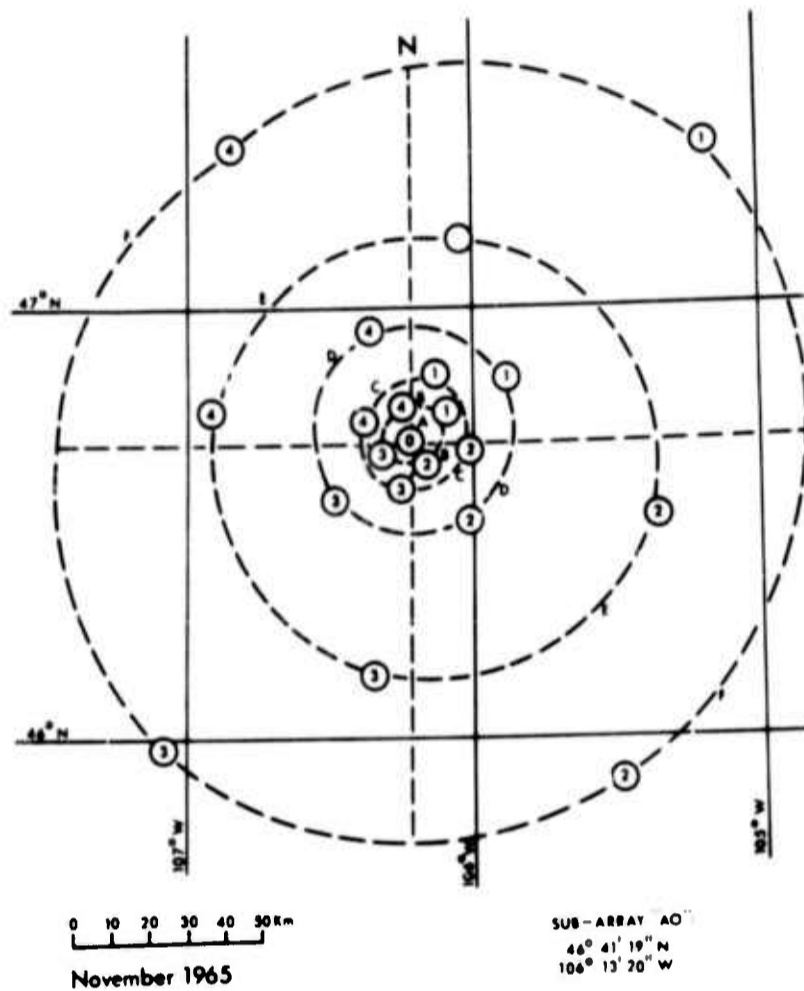
LASA

NAME	AZIMUTH	DELTA-KM	THETA	X	Y
B1	54.902	12.312	35.098	10.07330	7.07912
B2	141.477	7.614	308.523	4.74223	-5.95686
B3	246.010	8.039	203.990	-7.34456	-3.26849
B4	347.011	9.063	102.989	-2.03704	8.83111
C1	23.531	18.291	66.469	7.30259	16.77000
C2	97.459	16.245	352.541	16.10754	-2.10883
C3	191.498	12.981	258.502	-2.58753	-12.72050
C4	294.023	12.769	155.977	-11.66298	5.19829
D1	56.459	30.497	33.541	25.41896	16.85062
D2	141.708	26.250	308.292	16.26637	-20.60261
D3	232.156	25.110	217.844	-19.82894	-15.40536
D4	336.360	30.753	113.640	-12.33163	28.17229
E1	13.507	54.221	76.493	12.66405	52.72133
E2	106.254	68.551	343.746	65.81109	-19.18699
E3	188.314	60.556	261.686	-8.75616	-59.91960
E4	278.849	53.706	171.151	-53.06676	8.26157
F1	45.670	109.262	44.330	78.15803	76.35121
F2	146.491	103.543	303.509	57.16296	-86.33393
F3	220.066	103.487	229.934	-66.61130	-79.19908
F4	325.943	97.244	124.057	-54.45840	80.56474

Figure I-1. Subarrays and Coordinates (Relative to A0)

- Power-density spectra show peaks which vary between 0.05 and 0.07 Hz and also between 0.11 and 0.14 Hz. These regions are consistent with the regions of high coherence.

- Most horizontal and some vertical instruments show a peak in the region below 0.05 Hz. Where the horizontal instruments show a peak but the vertical instruments do not, the horizontal components contain about 15 db more power than the vertical components.

- Most horizontal sensors are about 3 db noisier than the vertical sensors in the 0.1- to 0.2-Hz region.

- Power spectra of similar components are generally space-stationary.

- The average power level of summer noise is about 0 to 3 db lower than the quiet winter noise.

- Noise peaks in the wavenumber spectra sometimes agree with the low regions in the surface weather map. However, there are cases when there is no correlation between noise peaks and low-pressure centers.
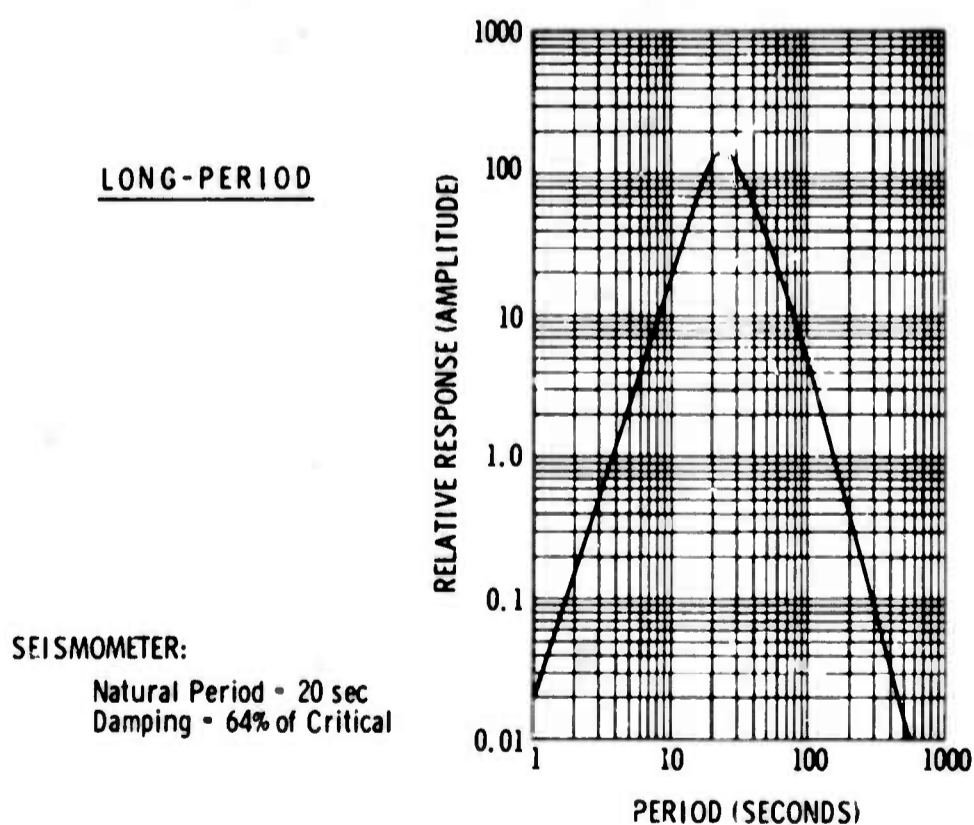
LONG-PERIOD

SEISMOMETER:
Natural Period = 20 sec
Damping = 64% of Critical

Figure I-2. Response of Instrument-Amplifier-Filter Combination

science services division

SECTION II
DATA PROCESSING

The data consisted of eight 80-min noise samples recorded between 29 March and 7 October 1967 (Table II-1). Four of these samples were recorded consecutively, forming a 320-min long noise sample. Data were resampled in the ratio of 5:1. Thus, the resulting sample rate was 1.0 sec, which corresponds to the Nyquist folding frequency of 0.5 Hz. No antialiasing was necessary, as the recording system has an effective cutoff below 0.5 Hz (Figure I-2).

The processing sequence consisted of despiking; removal of means; forming wiggly-trace playbacks; and computing power-density spectra, multiple coherences and wavenumber spectra. Data were despiked by linearly interpolating between the points immediately before and after the spike region. Wiggly-trace playbacks were used for quality control. Dead or wild traces were not included in the analysis. Overall, about 80 percent of the data was usable.

Power-density spectra were computed by using the maximum-entropy spectral-analysis technique.[2] Power-density spectra of seismic data were calibrated to ground motion by using conversion factors of 375 digital units/μ for vertical instruments and 400 digital units/μ for horizontal instruments.

Spectral matrices used for the multiple coherence and wavenumber spectral estimates were obtained by taking the fast Fourier transforms of 4096-point segments, setting $\varphi_{ij} = F_i^* F_j$, and smoothing over adjacent frequencies. The amount of smoothing depended upon the type of analysis to be done and the number of channels involved. Additional degrees of freedom were available for the long noise sample (four back-to-back tapes) by averaging transforms from all tapes.

Table II-1
NOISE SAMPLES

Date	Time Interval		
29 March 1967	5:31:26.6	to	6:49:59.6
11 May 1967	5:39:59.8	to	5:59:59.2
24 June 1967	2:11:59.9	to	3:31:59.3
24 June 1967	3:31:59.9	to	4:51:59.3
24 June 1967	4:51:59.9	to	6:11:59.3
24 June 1967	6:11:59.9	to	7:31:59.3
10 July 1967	2:26:00.1	to	3:45:59.5
7 October 1967	13:34:59.6	to	14:54:59.0

Prediction error was computed from the multiple coherences as a function of frequency. (Prediction error is the normalized power in the reference channel which cannot be predicted by linear least-mean-square-error filters from the other channels and is equal to $|1 - (\text{coherence})|$.)[3] Wavenumber spectra were computed by the conventional technique, which is equivalent to beamsteering and integrating the output power in the frequency domain.

Additional processing was done on the 320-min noise sample to study the vertical component of the long-period noise. This processing consisted of forming the residual vertical-component covariance matrix conditioned on knowing the horizontal sensor outputs. The resulting covariance matrix was analyzed for coherences and spatial organization.

The F-ring was excluded in the long-noise-sample processing. Of the remaining 17 subarrays, only 12 had all three components usable on the four segments of the long noise sample. These subarrays were B2, B3, B4, C1, C3, C4, D1, D2, D3, D4, E1, and E4. Thus, 12 vertical and 24 horizontal channels were used in the analysis. The computational steps are summarized in the following paragraphs.

A 36x36 covariance matrix, formed by the vertical and horizontal sensors, was obtained. Each element, $\varphi_{ij}(f)$, of this matrix was calculated by averaging the crosspower between the ith and j^{th} sensors over about 80 adjacent frequencies and over the four consecutive time segments also.

The 36x36 covariance matrix was partitioned into the following submatrices

$$\left[\begin{array}{c|c} \Omega_{VV} & \Omega_{VH} \\ \hline \Omega_{HV} & \Omega_{HH} \end{array} \right]$$

where

Ω_{VV} is the 12x12 crosspower matrix due to vertical sensors only

Ω_{VH} is the 12x24 crosspower matrix due to vertical and horizontal sensors

$\Omega_{HV} = (\Omega_{VH})^T$, where T represents conjugate transpose

Ω_{HH} is the 24x24 crosspower matrix due to horizontal sensors only

A 12x12 conditional covariance matrix Ω_{VV-H} of verticals, given the horizontals, was calculated by subtracting from Ω_{VV} that component which is predictable from the horizontal sensors. Thus,

$$\Omega_{VV-H} = \Omega_{VV} - \Omega_{VH} \, \Omega_{HH}^{-1} \, \Omega_{HV}$$

Prediction error and wavenumber analysis was done on Ω_{VV}, Ω_{HH} and Ω_{VV-H}. Also, prediction error was obtained in the case of horizontal sensors predicting the vertical sensor outputs.

BLANK PAGE

SECTION III
RESULTS OF DATA PROCESSING

Results are presented in chronological order except for the long noise sample (24 June 1967) which is presented first. Playback sections, power spectra, prediction-error curves, and wavenumber spectra are presented for each noise sample. Maps of surface weather and waveheight charts from the nearest available time are also shown. Coherence between microbarograph and long-period seismometer data is discussed in Section IV.

It is generally considered that the microseism peaks near 0.13 Hz should not be included in the band of long-period data analysis aimed at discrimination. Therefore, except for the long noise sample, $\vec{f-k}$ spectra were computed and studied for only the 0.05- to 0.08-Hz peak.

A. 24 JUNE 1967 LONG NOISE SAMPLE

Figures III-1 through III-4 show four 20-min sections taken from the four noise-sample tapes. This is the quietest sample analyzed, winter or summer. Table III-1 shows the rms levels of the noise samples presented in this report and, for comparison, the levels of three previously studied winter samples.[1]

Table III-1

NOISE-SAMPLE RMS VALUE

Date	RMS (Digital Units)
3 Dec 1966	20
13 Dec 1966	10
7 Feb 1967	33
29 Mar 1967	9
11 May 1967	6
24 Jun 1967	5
10 Jul 1967	7
7 Oct 1967	7

science services division

The power-density spectra (Figures III-5 through III-8) contain a major broad peak in the vicinity of 0.06 Hz and a very minor broad peak in the vicinity of 0.13 Hz. Generally, but not at every location, the horizontal components are considerably (5 to 15 db) noisier than the vertical components below about 0.06 Hz.

A sampling of prediction-error results (Figure III-9) shows that most of the noise coherence occurs in the 0.07-Hz peak. Figure III-10 shows the wavenumber spectra at 0.07 Hz for the vertical components, the north-south components, and the vertical residual components (residual after linear prediction using all horizontal elements). The spectra of the vertical and north-south components are generally similar. These spectra show that at 0.07 Hz (Figure III-10) the energy is widely distributed but arrives from three main directions (N72°W, N80°E and S20°W) and propagates at 3.5 km/sec.

The wavenumber spectrum of the vertical-component residuals shows relative peaks in roughly the same areas but is more "white" in the region of seismic noise (V > 3 km/sec).

The residual vertical components are generally 3 to 6 db quieter than the vertical components (Figure III-9). This noise reduction is the result of "predicting off" some of the Rayleigh-mode energy common to both components. The remaining residual noise has significant coherence. Figure III-11 shows one example of the prediction error among the residual components. The low prediction error near 0.07 Hz indicates a considerable spatial organization.

From the f-$\vec{k}$ spectra (Figure III-9) it would appear that the residual noise field is probably a mixture of fairly isotropic surface-mode energy and P-wave energy, with the surface-mode energy dominant. Thus,

science services division

on the quietest noise sample analyzed, with the surface-mode energy further reduced 3 to 6 db by horizontal-vertical prediction, it appears that Rayleigh-mode energy still is dominant in the 16- to 18-sec microseism peak.

Figures III-12 and III-13 show surface atmospheric pressure and waveheights, respectively. There is no obvious correlation between the $\vec{f}-k$ spectra at 0.07 Hz and the wave activity or low-pressure areas.

Figure III-14 shows the $\vec{f}-k$ spectral estimate of the vertical and residual vertical components at 0.13 Hz. The plot for the residual vertical components has a higher edge velocity (5 km/sec vs 2 km/sec). These two spectra are essentially the same. The vertical components showed almost no reduction when conditioned on the horizontal components at 0.13 Hz. It is recalled from the power spectra (Figures III-5 through III-8) that the power density is very low in this region and is only a few db above system (including digitization) noise.

The wavenumber spectra indicate that the noise is dominated by a peak coming from the north at very high velocity (V > 20 km/sec). It appears that on this very quiet day the noise near 0.13 Hz is dominated by mantle P-wave energy. This is the only time P-wave energy was observed on the LASA long-period data.

B. 29 MARCH 1967 NOISE SAMPLE

Table III-1 indicates that the 29 March 1967 sample is noisy for a summer sample, although it is considerably quieter than some winter samples.

The 20-min segments in Figure III-15 show a burst of noise with a dominant 0.06-Hz frequency. This agrees with the 0.06-Hz peak in the power-density spectrum (Figure III-16). The power-density spectrum also shows multiple peaks below 0.05 Hz and a sharp peak at 0.13 Hz.

science services division

Figure III-17 shows several prediction-error results. The peaks near 0.06 and 0.13 Hz appear to be most coherent, and the coherence falls off below about 0.05 Hz. There is good coherence between the vertical component and nearby horizontal components in the spectral peaks. This indicates that the peaks are Rayleigh-mode energy.

Figure III-18 shows the wavenumber spectra of the vertical and north-south components at 0.06 Hz. The vertical component's spectrum indicates Rayleigh-mode energy from areas with bearings N 80°W and N 70° E. The north-south component spectrum shows the same peaks but is more complex. There is a good agreement between the azimuths of the peaks at 0.06 Hz in the wavenumber spectrum and the low regions on the surface weather map (Figure III-19).

Figures III-20 and III-21 show the wave activity at 00.00 hr and 12.00 hr, respectively. Both show intense wave activity along the Newfoundland coast but only the latter shows high wave activity along the British Columbian coastline. The noise sample was taken around 06.00 hr. It seems likely that the high wave activity on the British Columbian and Newfoundland coasts was generating this 0.06-Hz noise.

C. 11 MAY 1967 NOISE SAMPLE

The 11 May 1967 noise sample (Figure III-22) comes from a fairly quite period, as can be seen from the low rms level in Table III-1. This agrees with the lack of wave activity on the continental coastlines (Figures III-23 and III-24).

Power-density spectra (Figure III-25) only show small high regions superimposed on a slowly decaying exponential curve. These high ill-defined regions are located below 0.05 Hz, around).07 Hz, and also in the vicinity of 0.13 Hz. Prediction-error plots (Figure III-26) show some

coherence between 0.03 and 0.07 Hz and also around 0.13 Hz; however, these coherences are not particularly high.

The vertical-component wavenumber spectra at 0.06 Hz (Figure III-27 show two peak regions — indicating that the energy is propagating as fundamental-mode Rayleigh-wave energy. The wavenumber spectrum for the east-west component indicates that the energy is distributed over a very wide azimuth. There is no obvious correlation between the azimuths of peaks in the wavenumber spectrum and the low regions in the surface weather map (Figure III-28).

D. 10 JULY 1967 NOISE SAMPLE

The 20-min segments (Figure III-29) show that about 40 percent of the horizontal channels were unusable. The vertical channels show a burst of noise with a dominant 0.06 Hz frequency.

The noise level (Table III-1) is fairly average for summer. The power-density spectra (Figure III-30) show three well-defined peaks: a single peak near 0.06 Hz and a double peak between 0.12 Hz and 0.16 Hz. There is also a fairly broad, high region below 0.05 Hz.

Prediction-error analysis (Figure III-31) on vertical sensors shows high coherence in the 0.05- to 0.07-Hz region and also at 0.15 Hz. Wavenumber spectral analysis (Figure III-32) shows fundamental-mode Rayleigh-wave energy propagating from the west. There is no obvious correlation between the direction of Rayleigh-wave energy as observed from the wavenumber spectrum and the surface weather map (Figure III-33). The waveheight chart (Figure III-34) does not indicate any significant activity near North American coastlines.

E. 7 OCTOBER 1967 NOISE SAMPLE

The 20-min segments (Figure III-35) show that about 35 percent of data (particularly B and E rings) were unusable.

The noise level (Table III-1) is fairly close to the summer average. Power-density spectra (Figure III-36) show two broad high regions around 0.07 Hz and 0.13 Hz.

Prediction-error analysis (Figure III-37) shows high coherence between vertical sensors at 0.07 Hz and 0.11 Hz, some coherence between vertical and horizontal sensors at 0.13 Hz, but little coherence between vertical and horizontal sensors at 0.07 Hz.

Wavenumber spectra at 0.06 Hz (Figure III-38) show energy propagating at about 3.5 km/sec and coming from two azimuths, e.g., N60°E and N60°W.

The surface weather map (Figure III-39) shows two important low regions located along the Newfoundland and Alaskan coasts. These locations correlate very well with the azimuth of the peaks in the wavenumber spectra.

The waveheight chart (Figure III-40) shows activity on the Newfoundland coast in the northeast, on the coast of Washington state in the west, and south of the Aleutians in the northwest. There is some correlation between the regions of wave activity and the azimuths of wavenumber peaks.

science services division
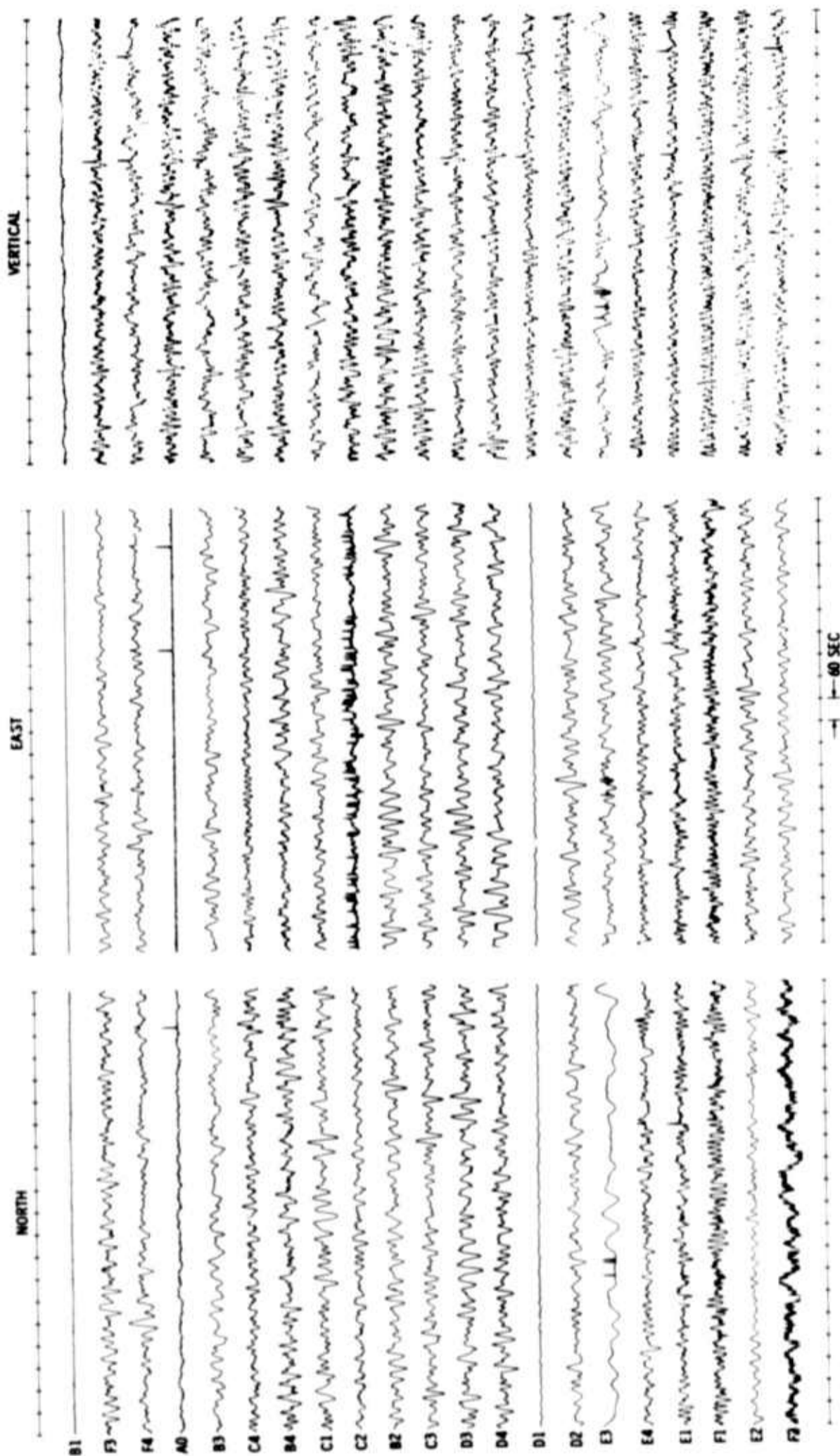
Figure III-1. Segment (2:11:59.9 to 3:31:59.3) of Long Noise Sample

science services division
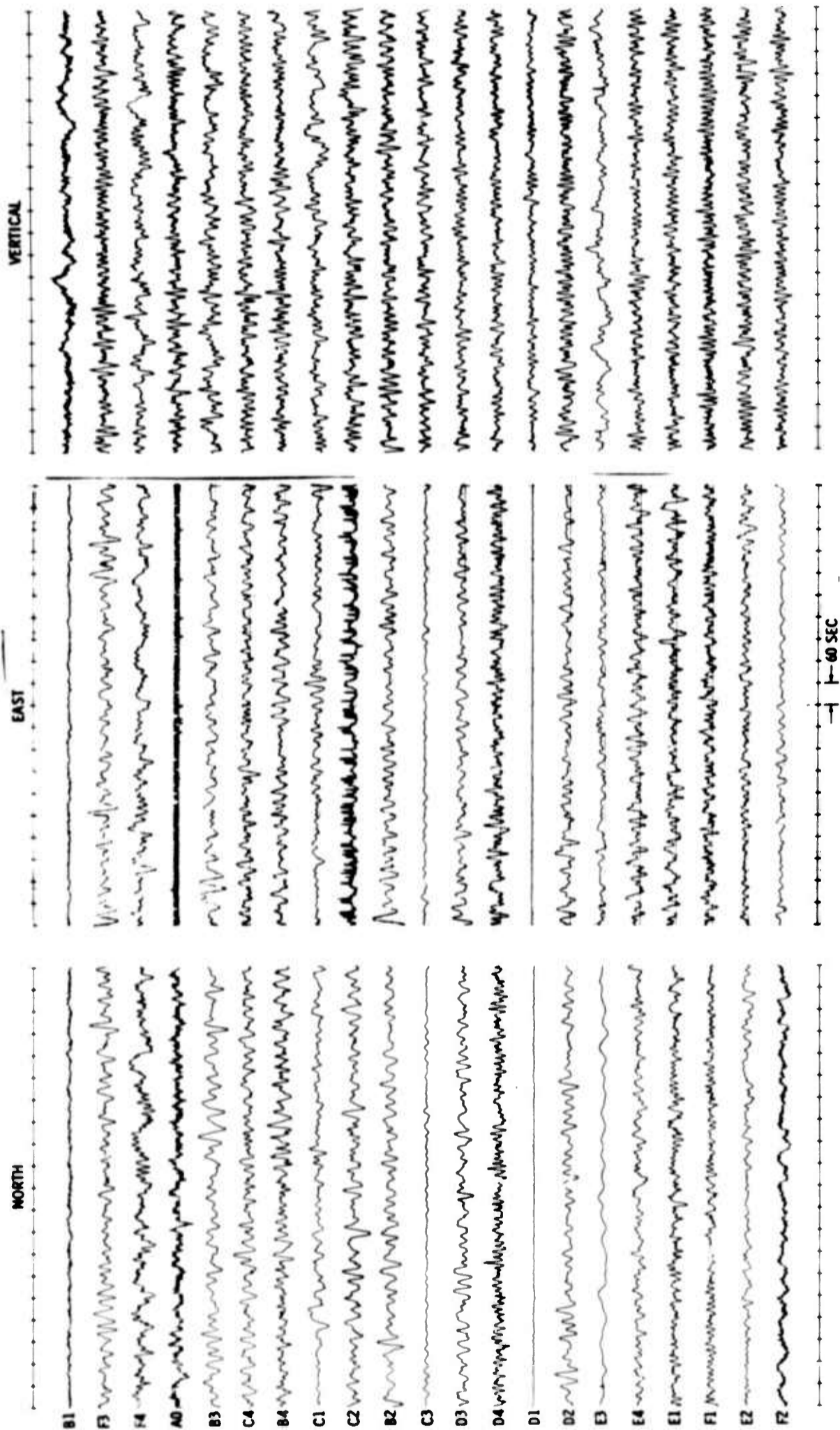
Figure III-2. Segment (3:31:59.9 to 4:51:59.3) of Long Noise Sample

science services division
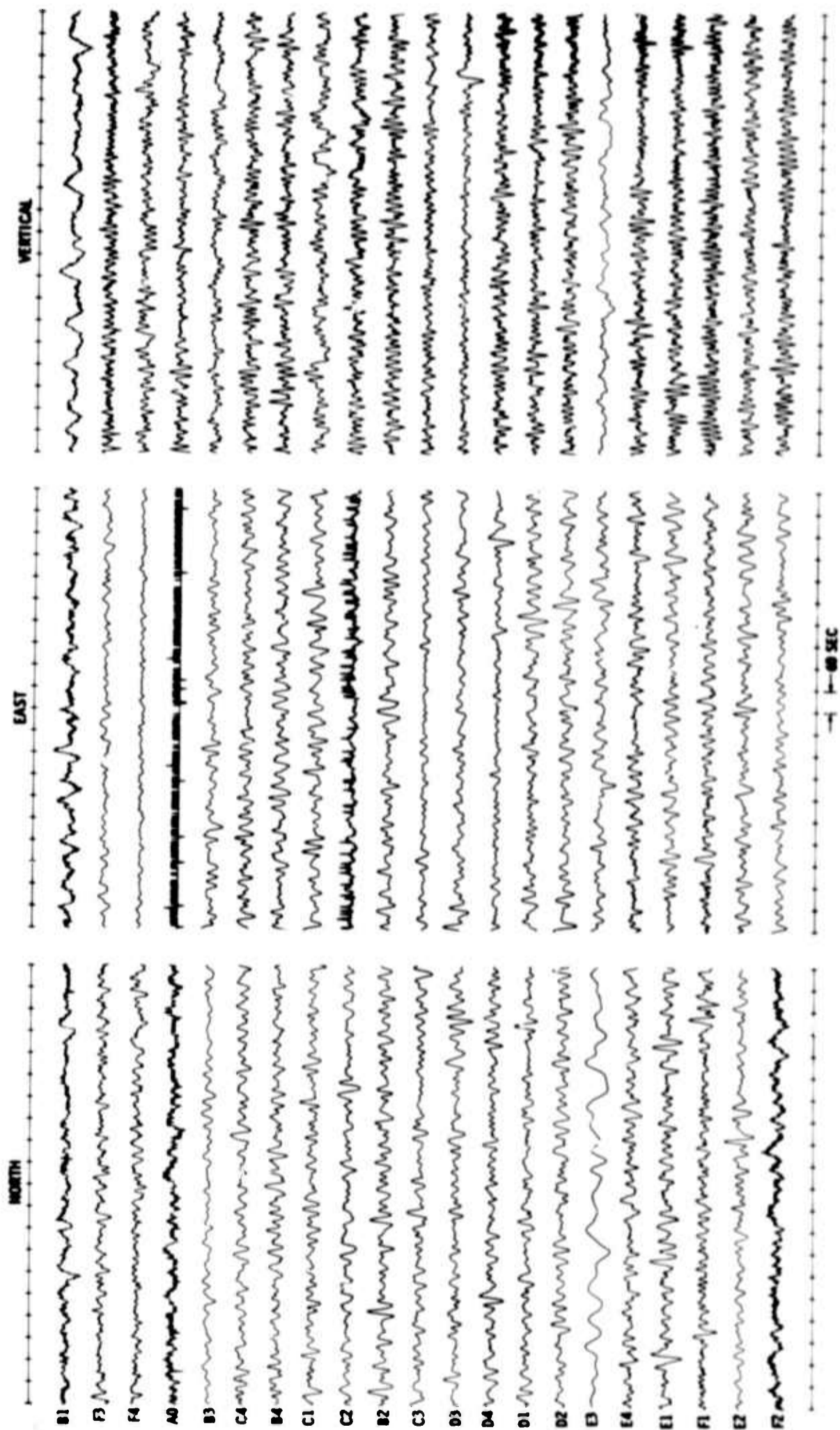
Figure III-3. Segment (4:51:59. 9 to 6:11:59. 3) of Long Noise Sample

science services division

Figure III-4. Segment (6:11:59.9 to 7:31:59.3) of Long Noise Sample
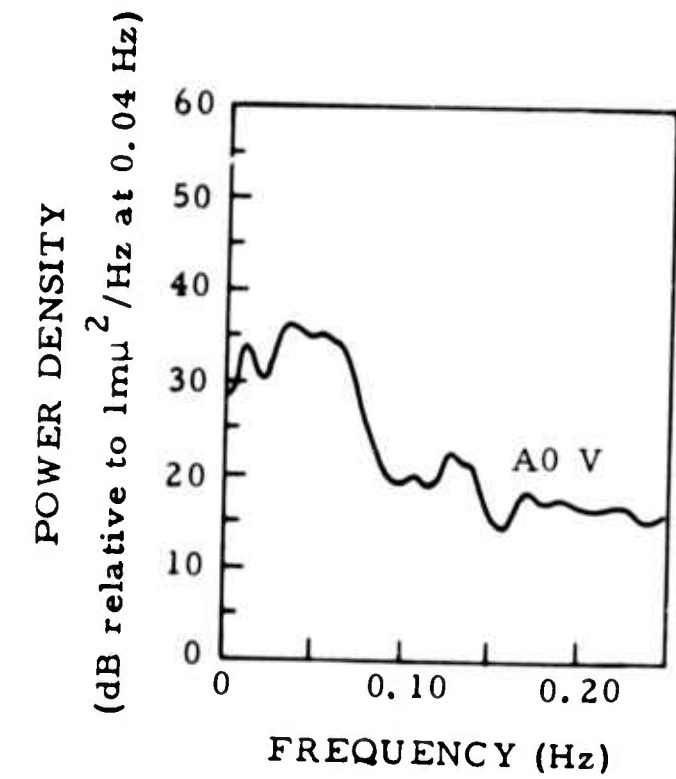
science services division
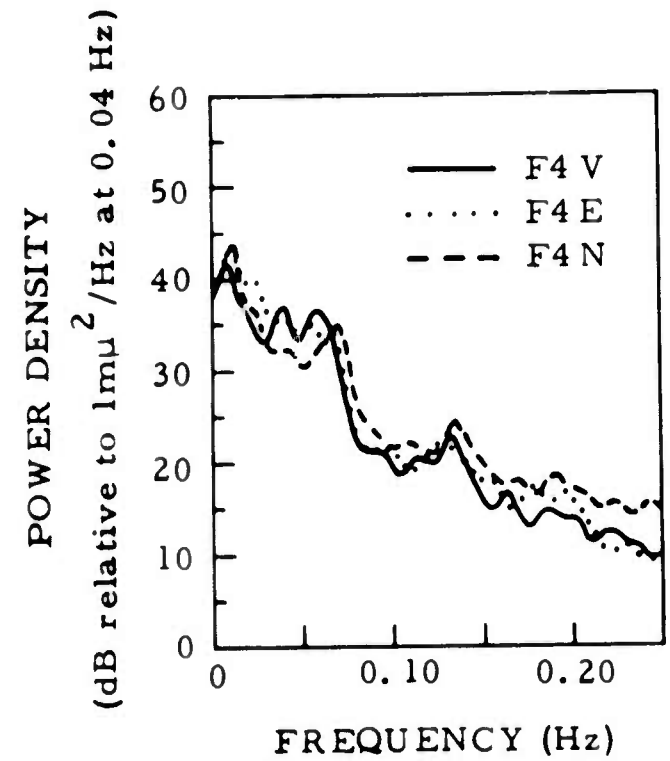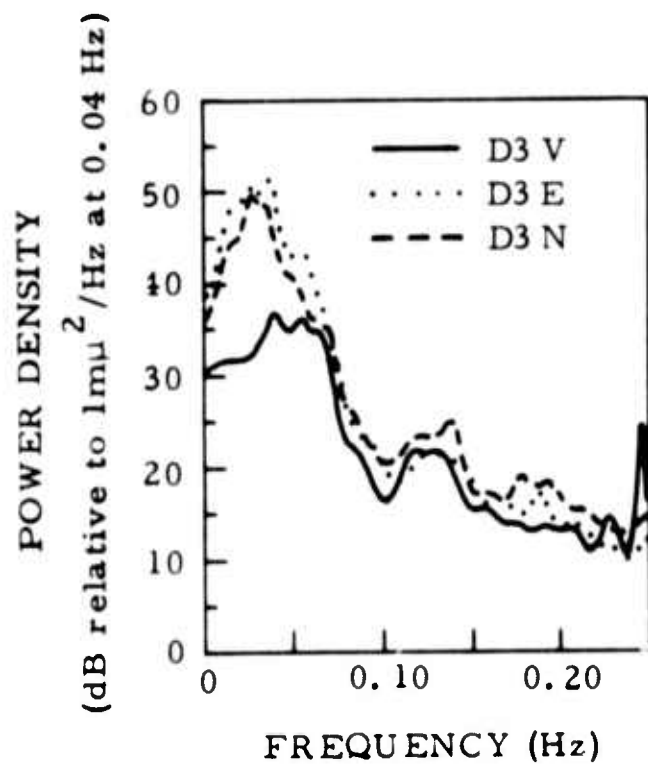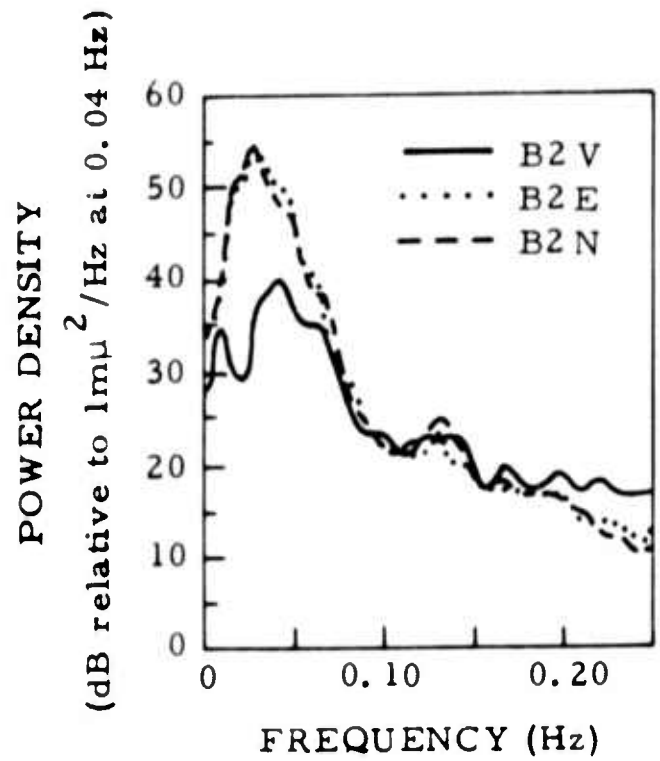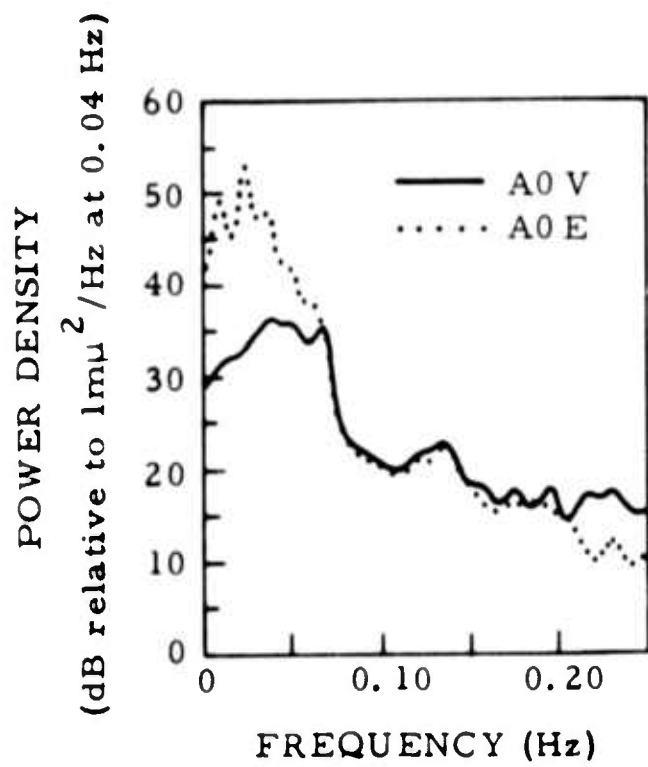
Figure III-5. Power-Density Spectra for Segment (2:11:59.9 to 3:31:59.3) of Long Noise Sample
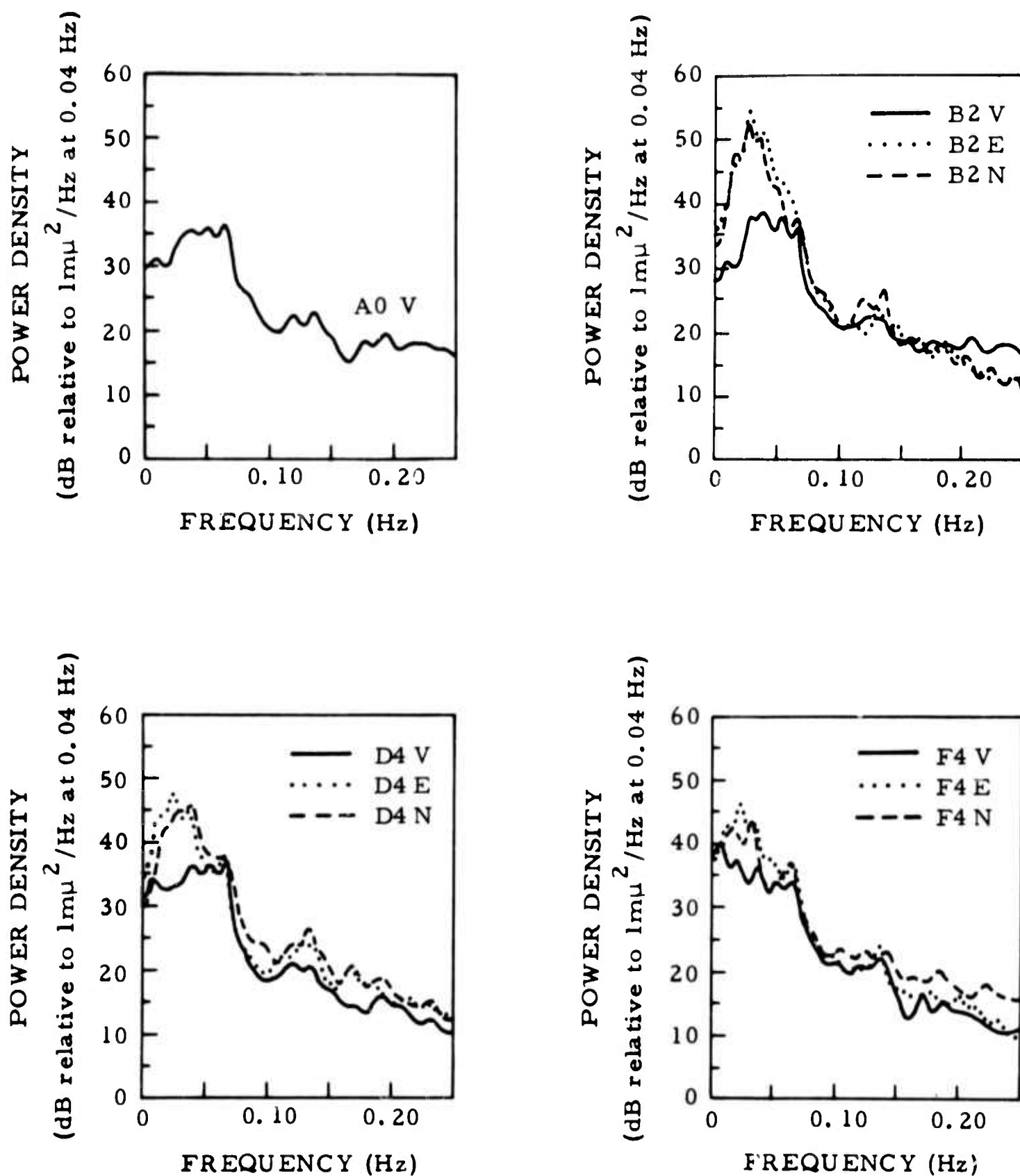
Figure III-6. Power-Density Spectra for Segment (3:31:59. 9 to 4:51:59. 3) of Long Noise Sample
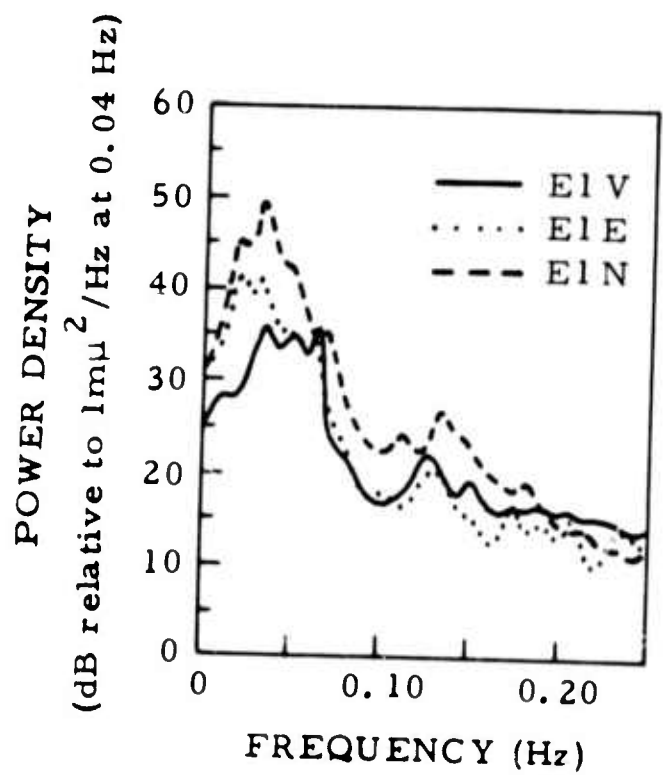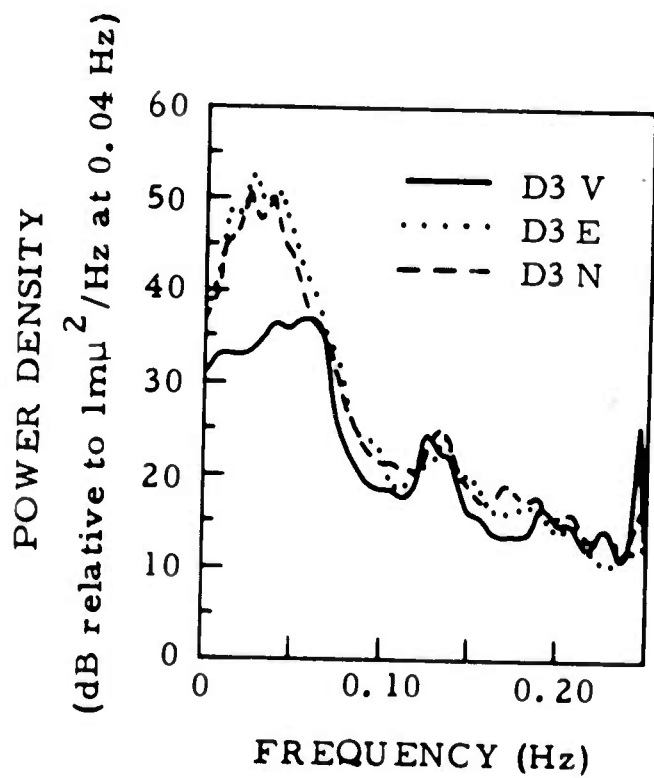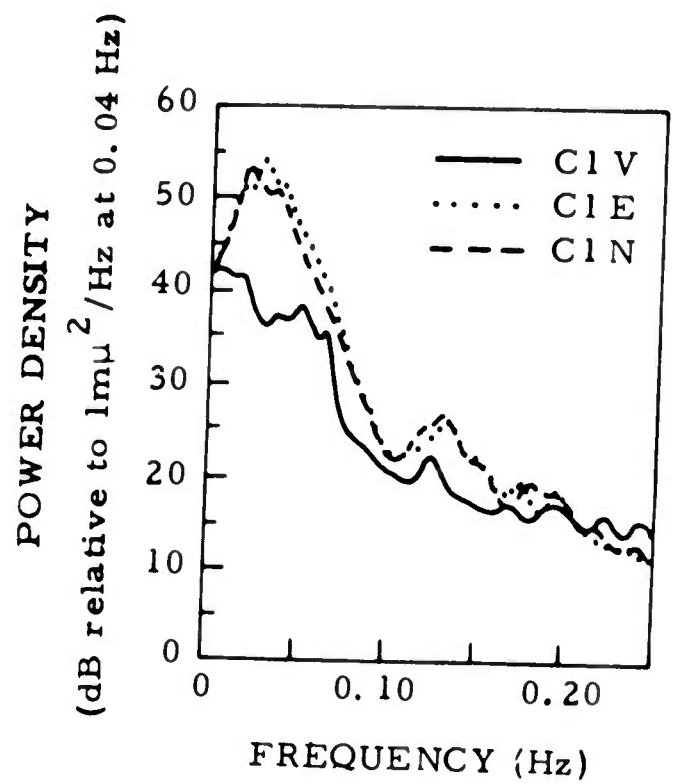
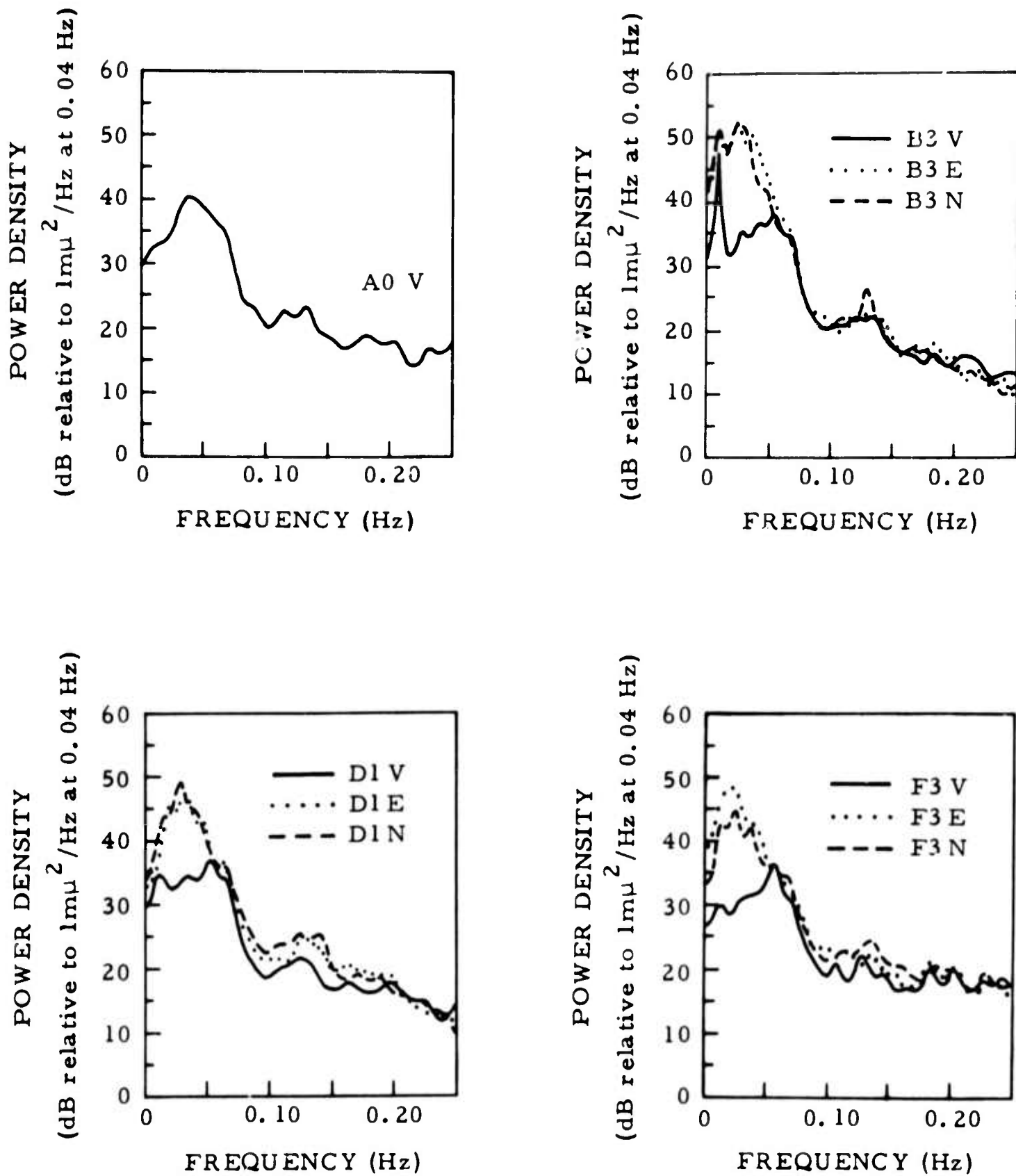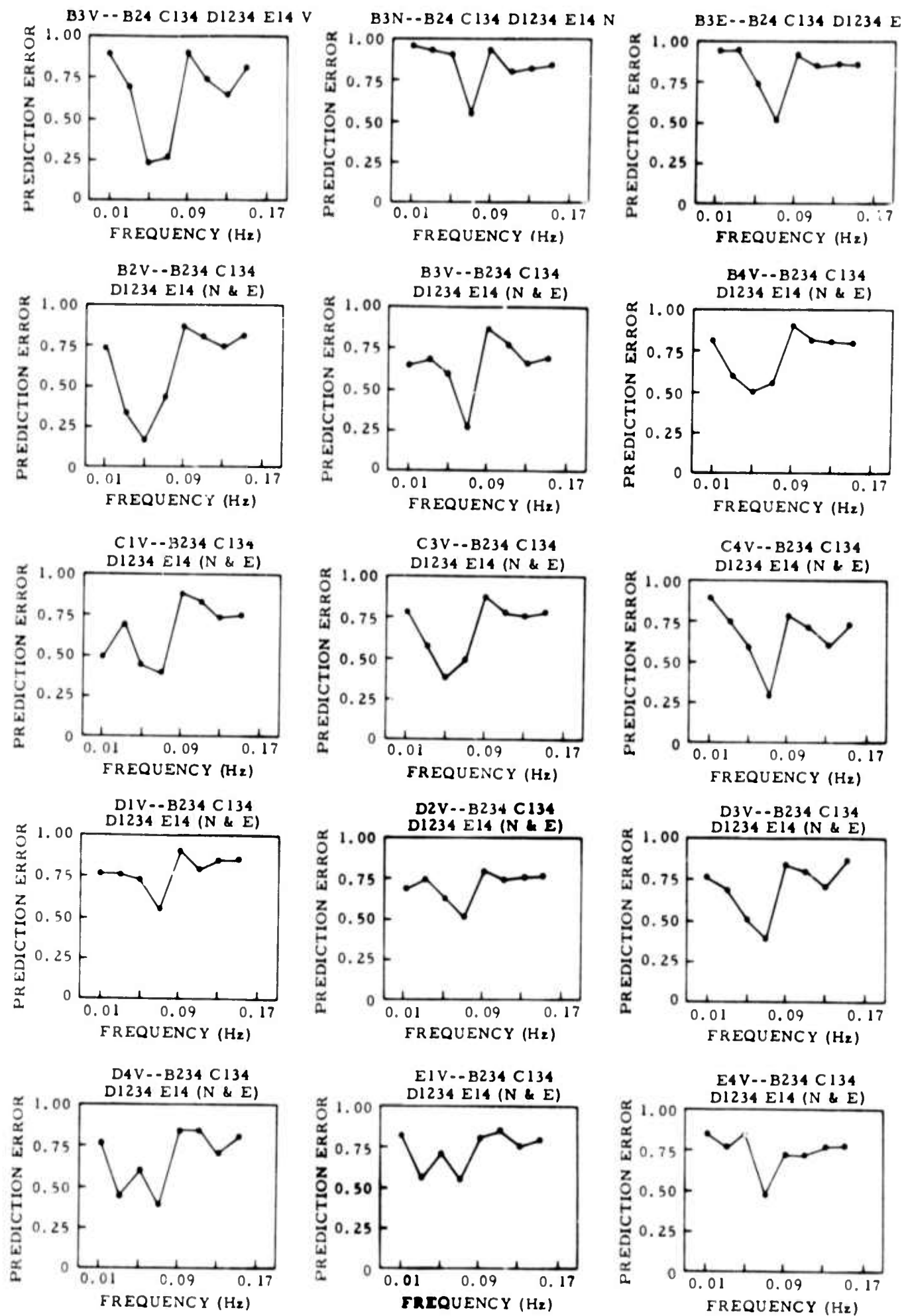Figure III-7.   Power-Density Spectra for Segment (4:51:59.9 to 6:11:59.3) of Long Noise Sample

science services division

Figure III-8.   Power-Density Spectra for Segment (6:11:59.9 to 7:31:59.3) of Long Noise Sample

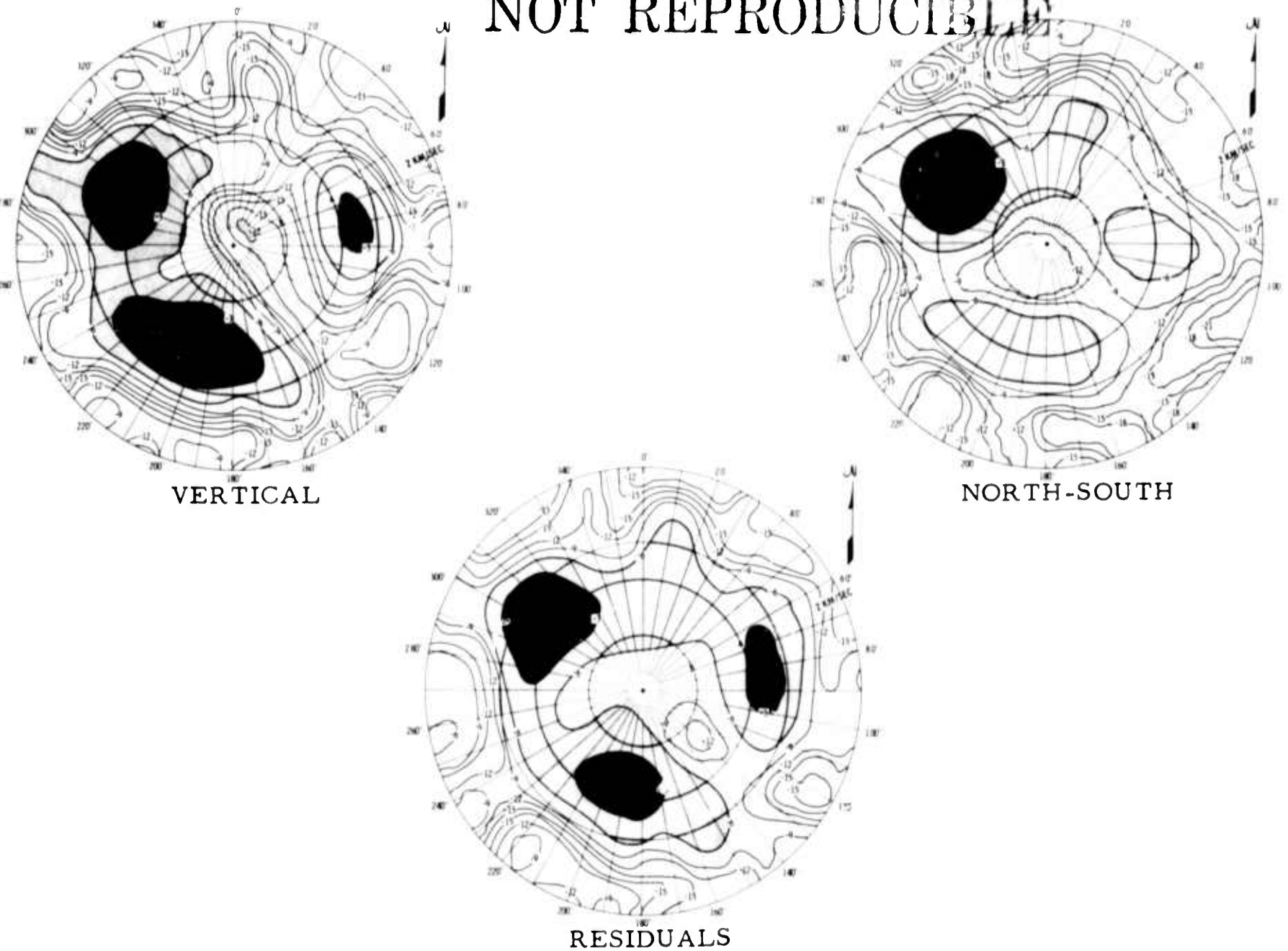Figure III-9.   Prediction-Error Plot for 24 June 1967
Long-Period Noise Sample

science services division

VERTICAL

NORTH-SOUTH

RESIDUALS

Figure III-10.   Wavenumber Spectra at 0.07 Hz, 24 June 1967
Long-Period Noise Sample

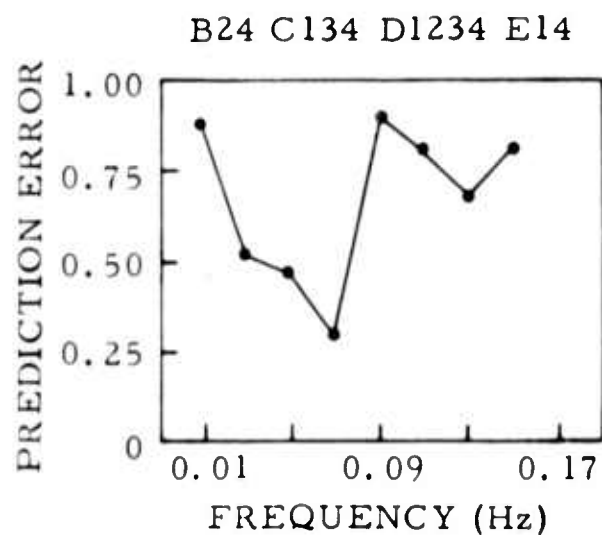B24 C134 D1234 E14

FREQUENCY (Hz)

Figure III-11.   Prediction-Error Plot for B3 Residual Minus
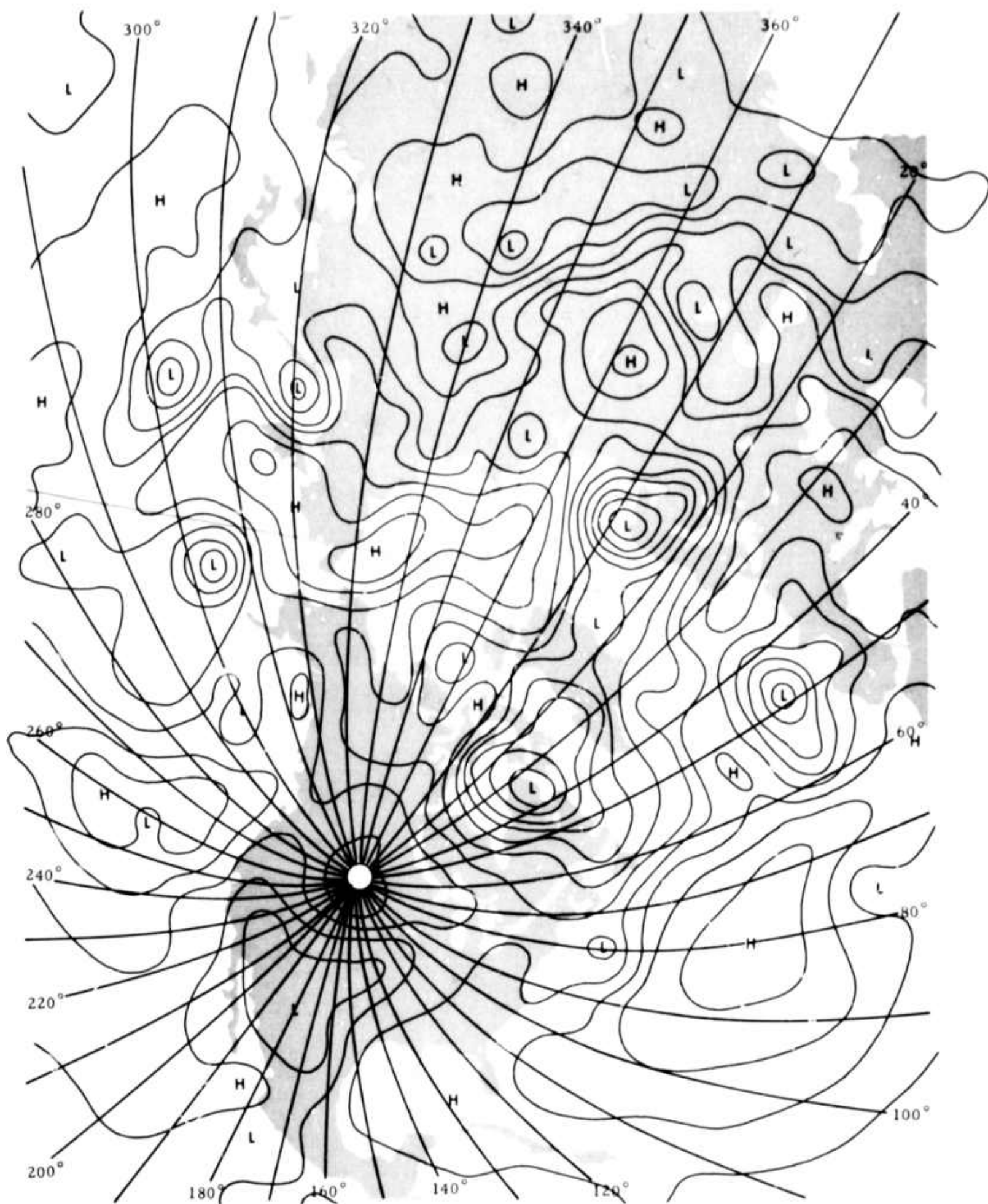(B2, B4, C1, C3, C4, D1, D2, D3, D4, E1, E4)

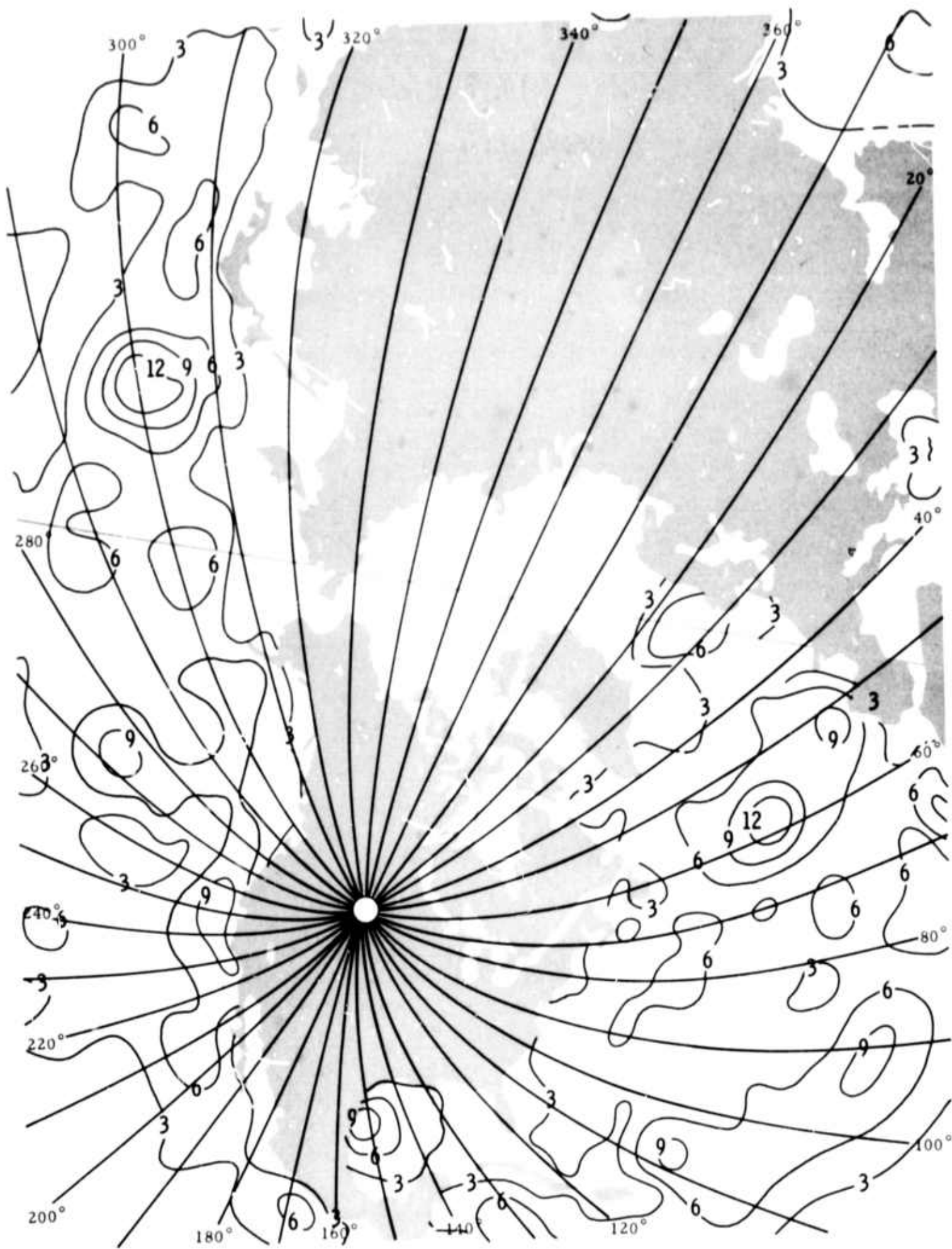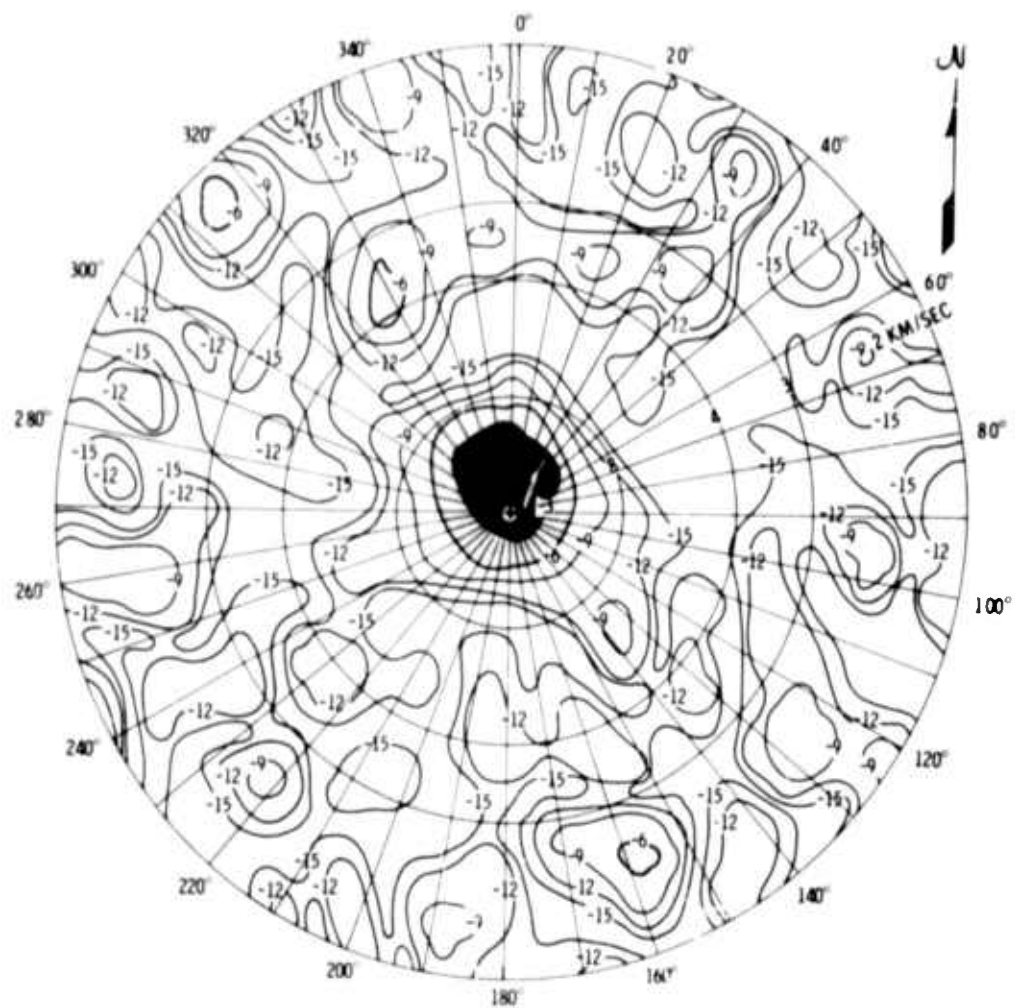Figure III-12.   Surface-Pressure Map at 06.00 Hr, 24 June 1967

Figure III-13. Waveheight Chart at 00.00 Hr, 24 June 1967
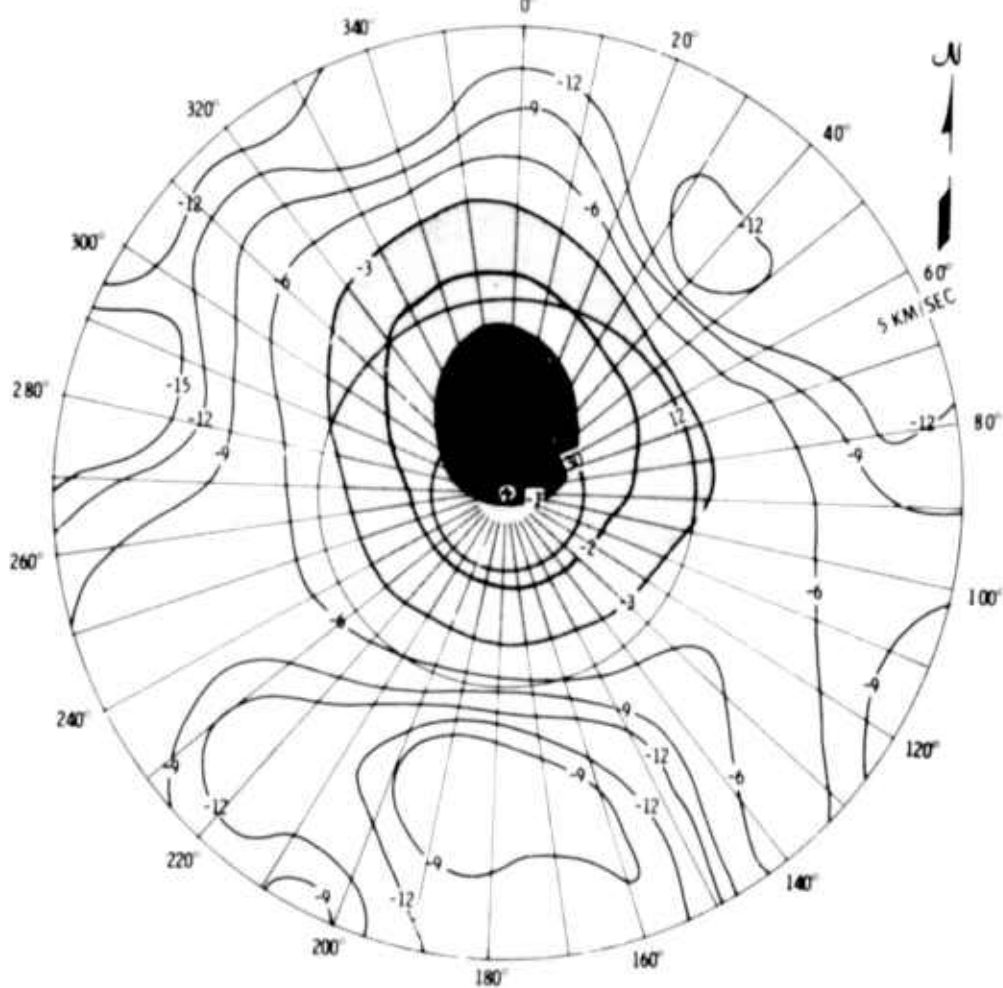
VERTICAL

RESIDUALS

Figure III-14. Wavenumber Spectra at 0.13 Hz, 24 June 1967
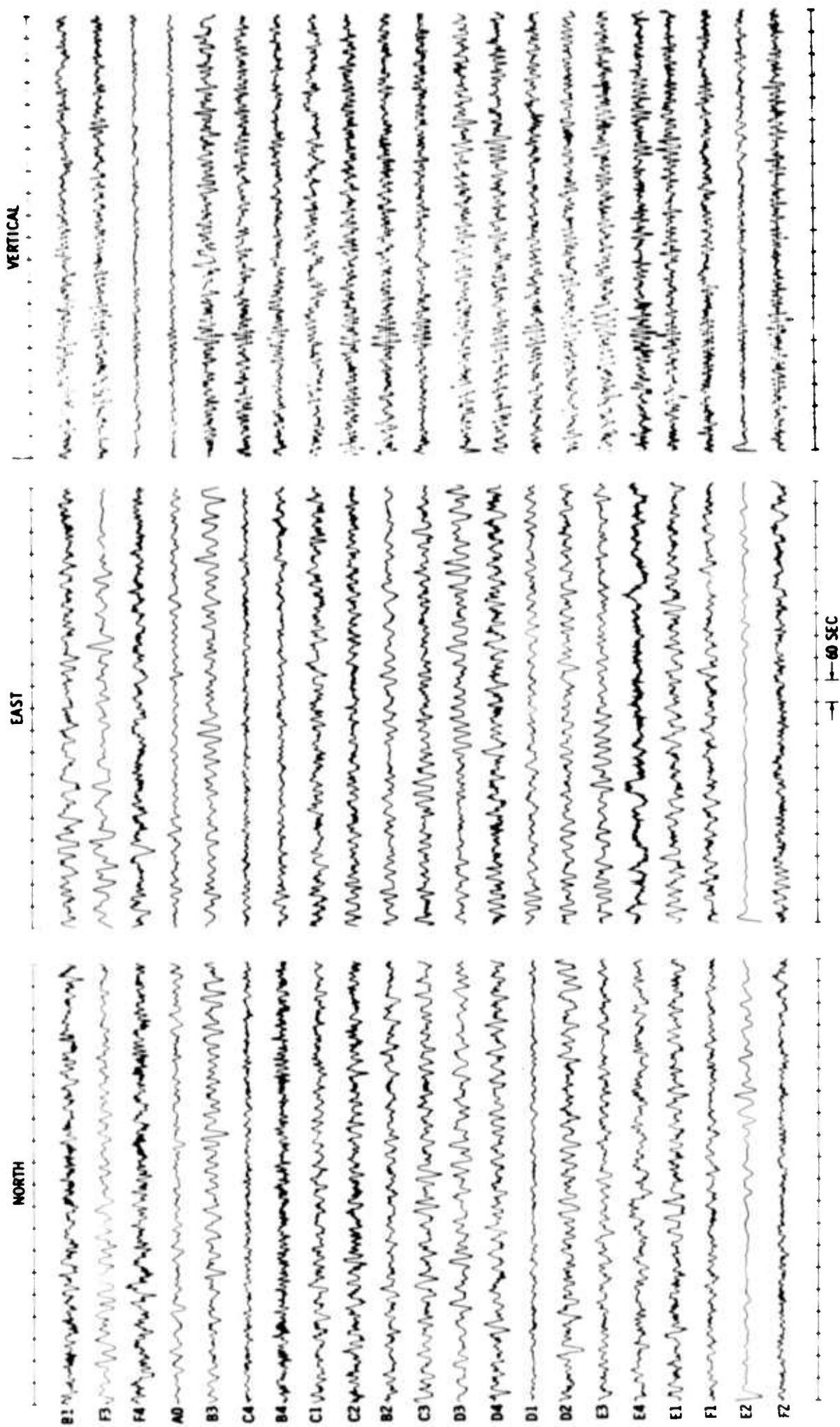Long-Period Noise Sample

Figure III-15. 20-Min Segments of 29 March 1967 Noise Sample
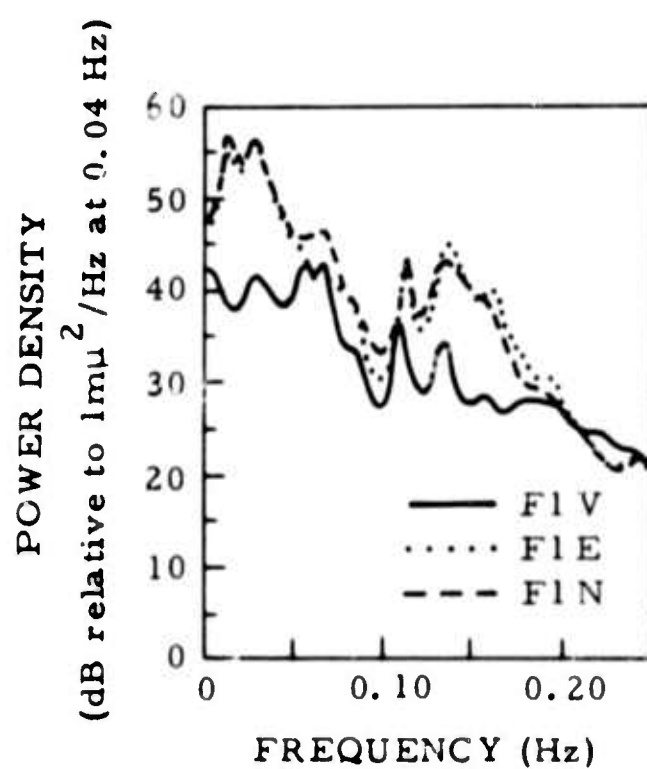
science services division
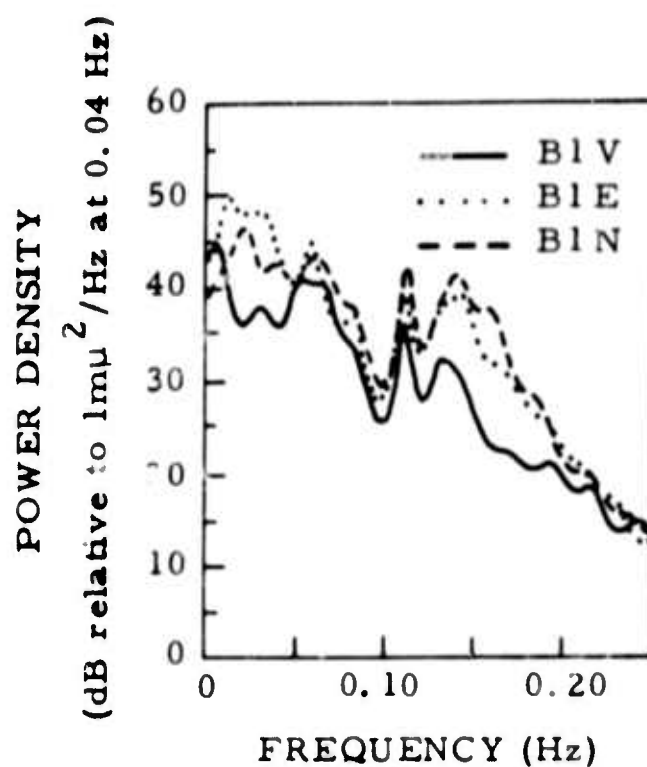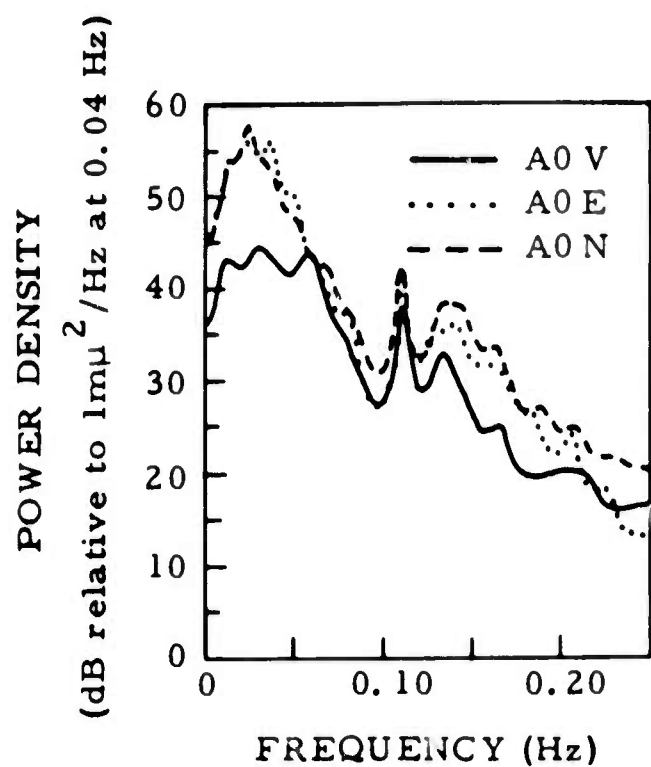
Figure III-16.   Power-Density Spectra of 29 March 1967 Noise

Figure III-17. Prediction-Error Plots for 29 March 1967 Noise Sample

science services division

VERTICAL

NORTH-SOUTH

Figure III-18. Wavenumber Spectra at 0.06 Hz, 29 March 1967 Noise Sample
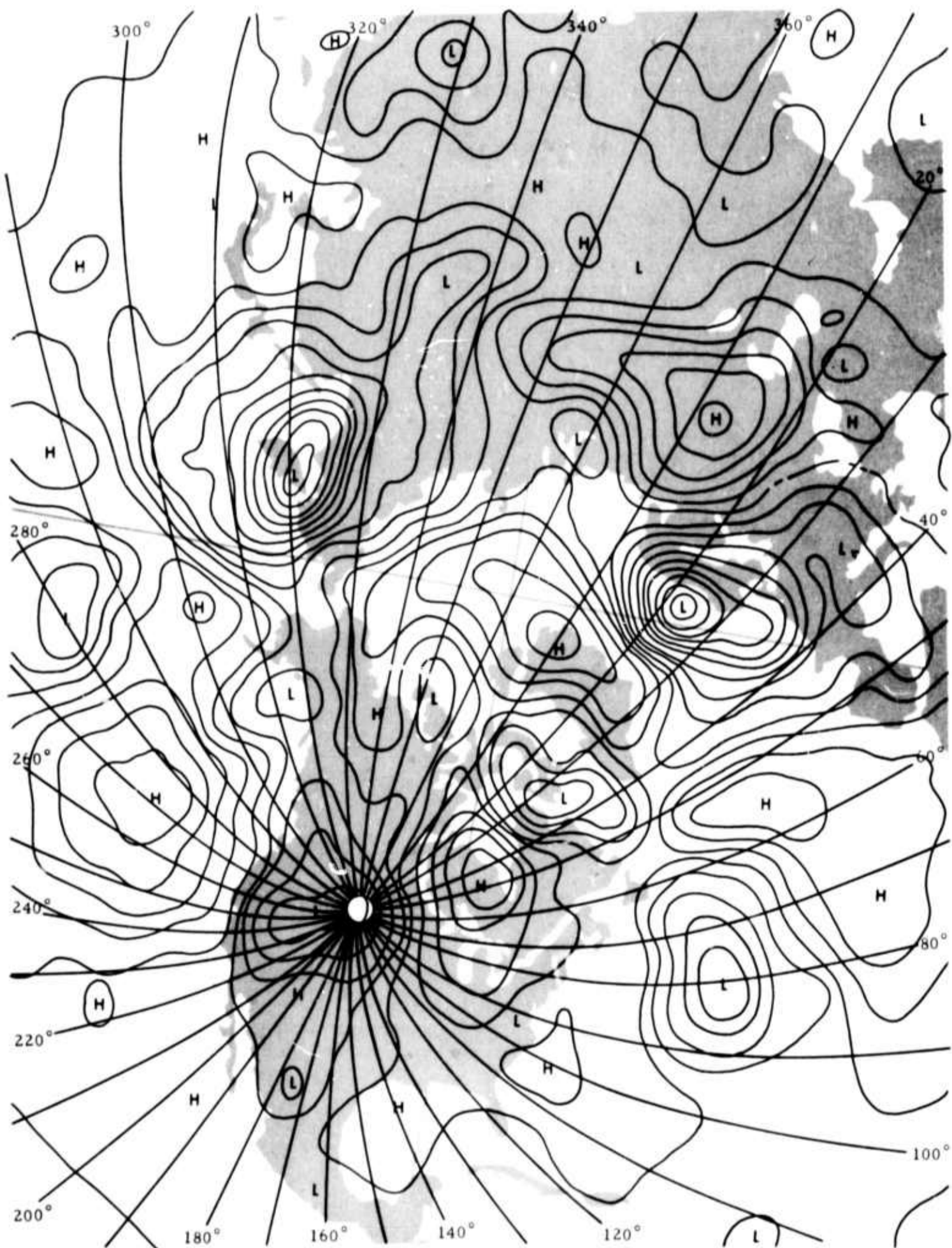
Figure III-19. Surface-Pressure Map at 06.00 Hr, 29 March 1967

science services division
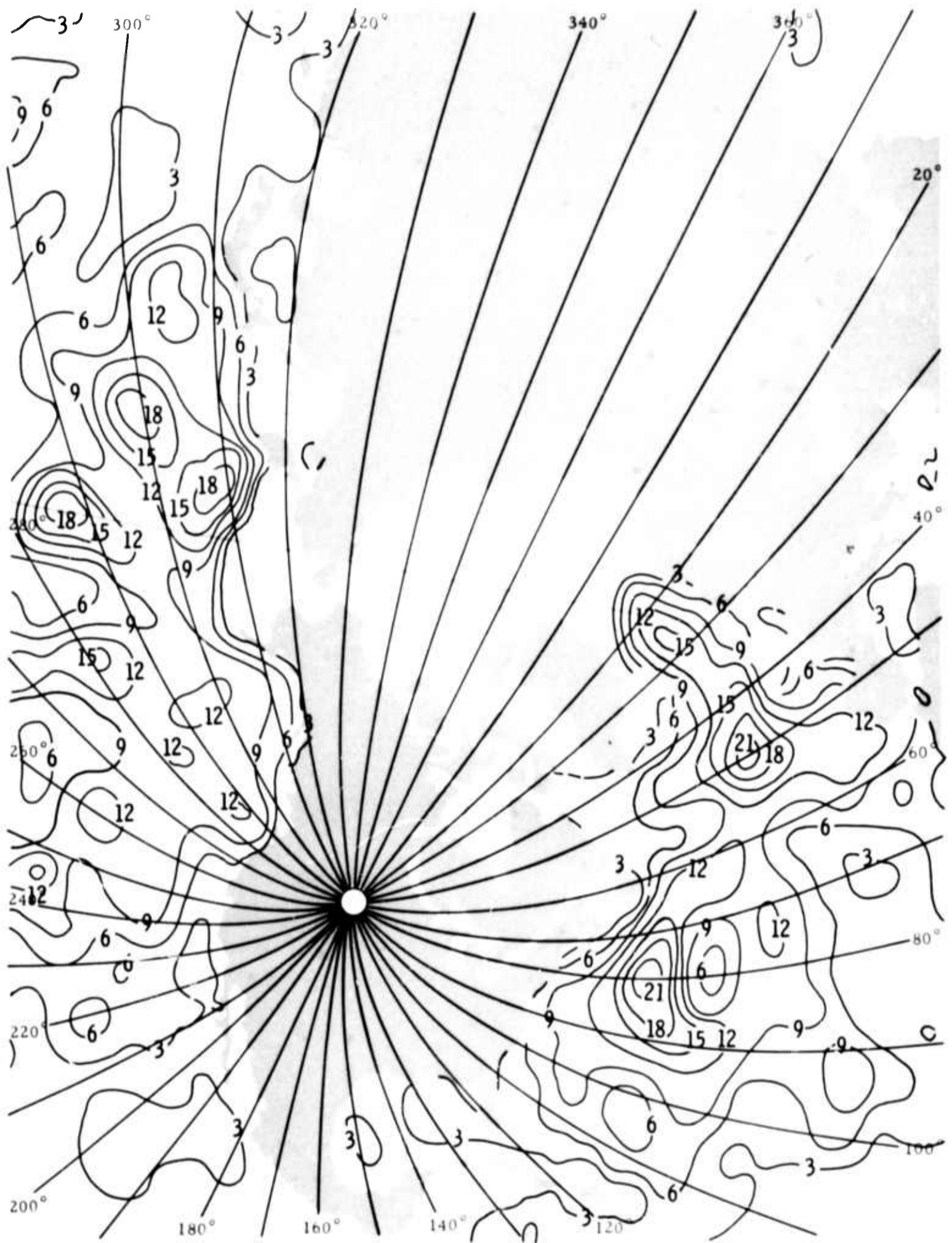
Figure III-20.   Waveheight Chart at 00.00 Hr. 29 March 1967

science services division
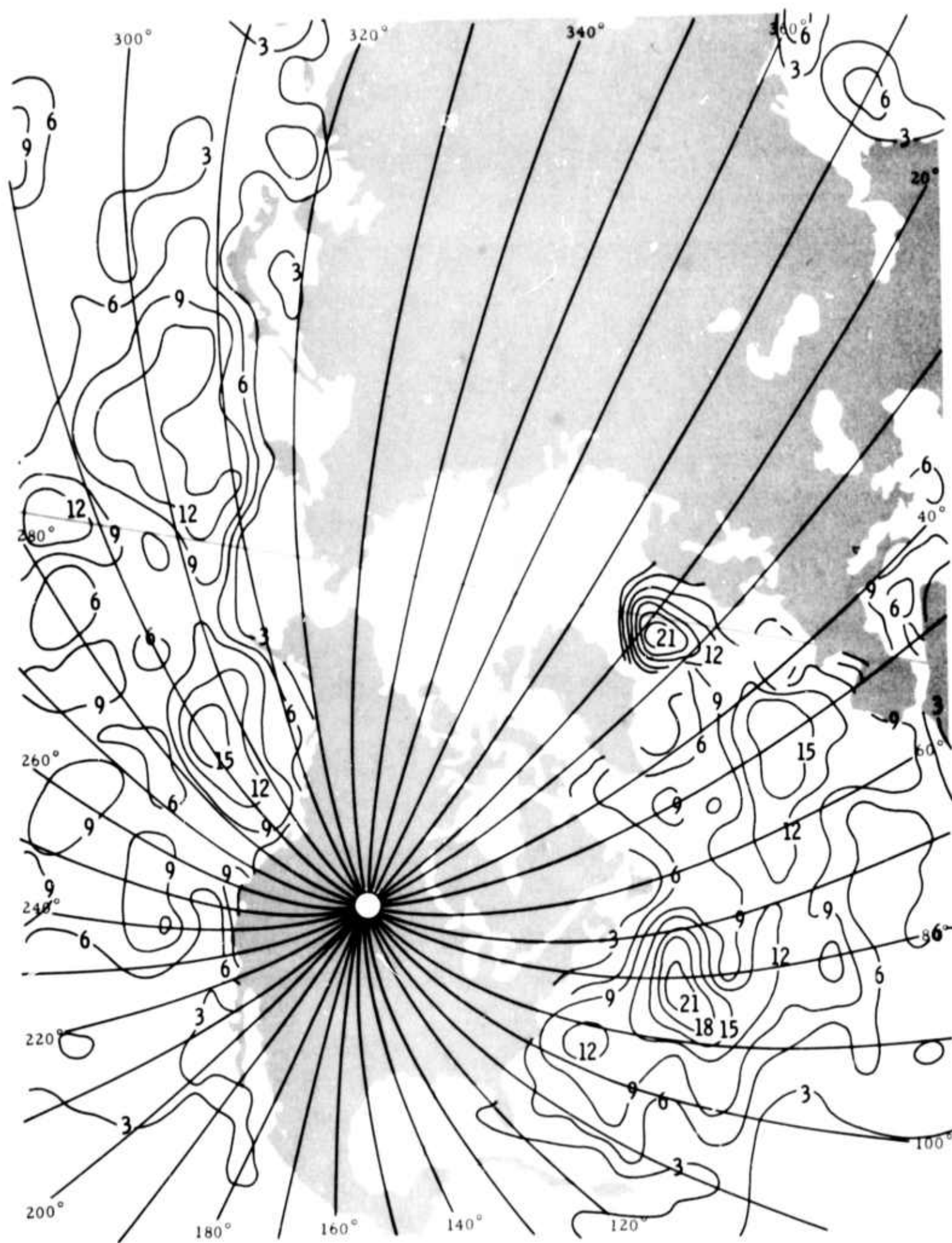
Figure III-21. Waveheight Chart at 12.00 Hr, 29 March 1967
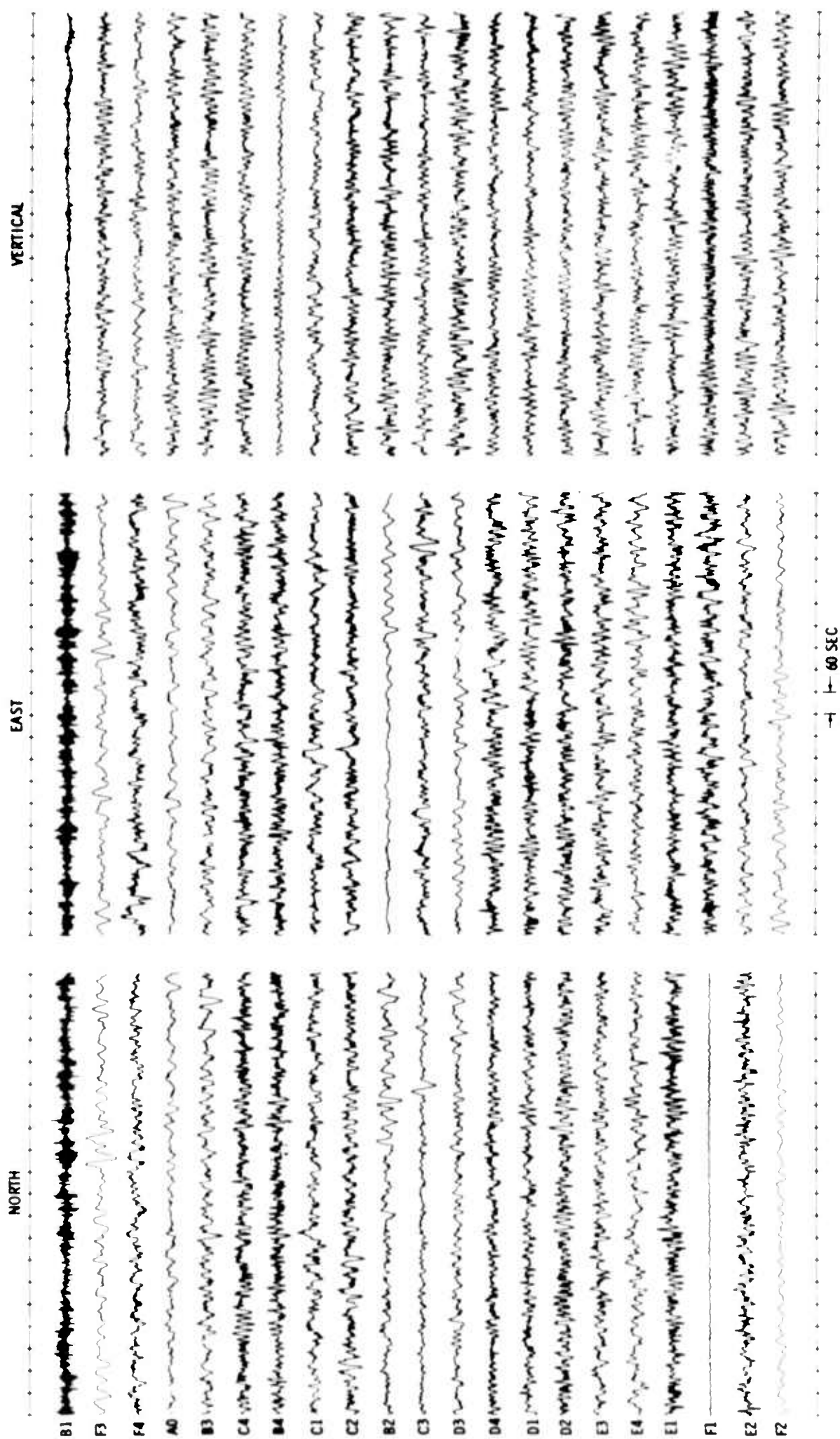
Figure III-22. 20-Min Segments of 11 May 1967 Noise Sample

science services division
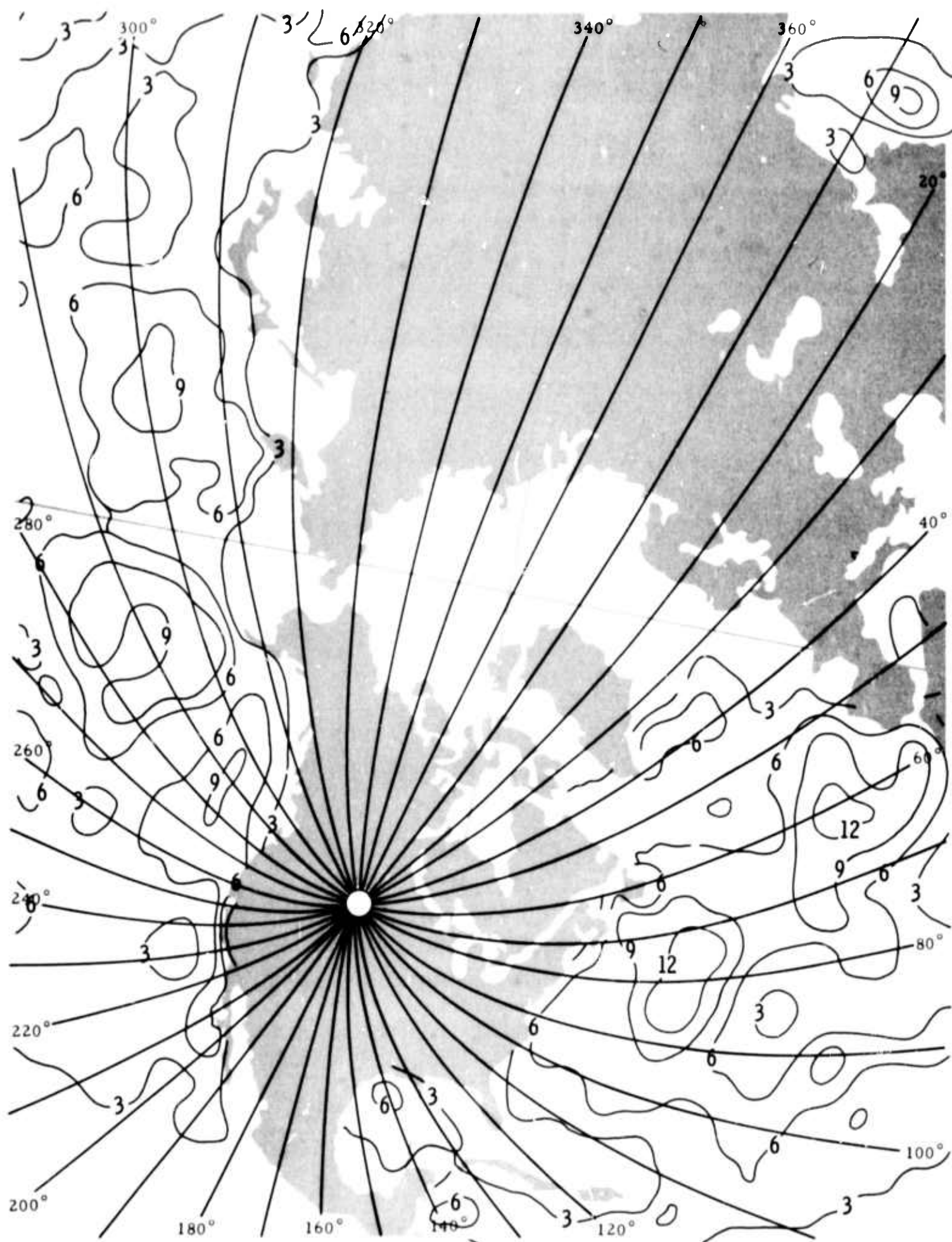
Figure III-23.   Waveheight Chart at 0.00 Hr, 11 May 1967
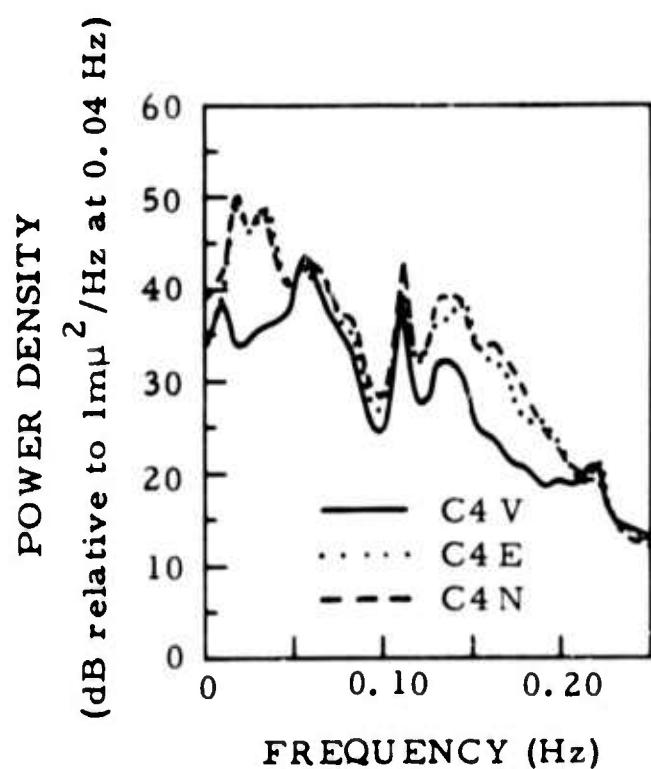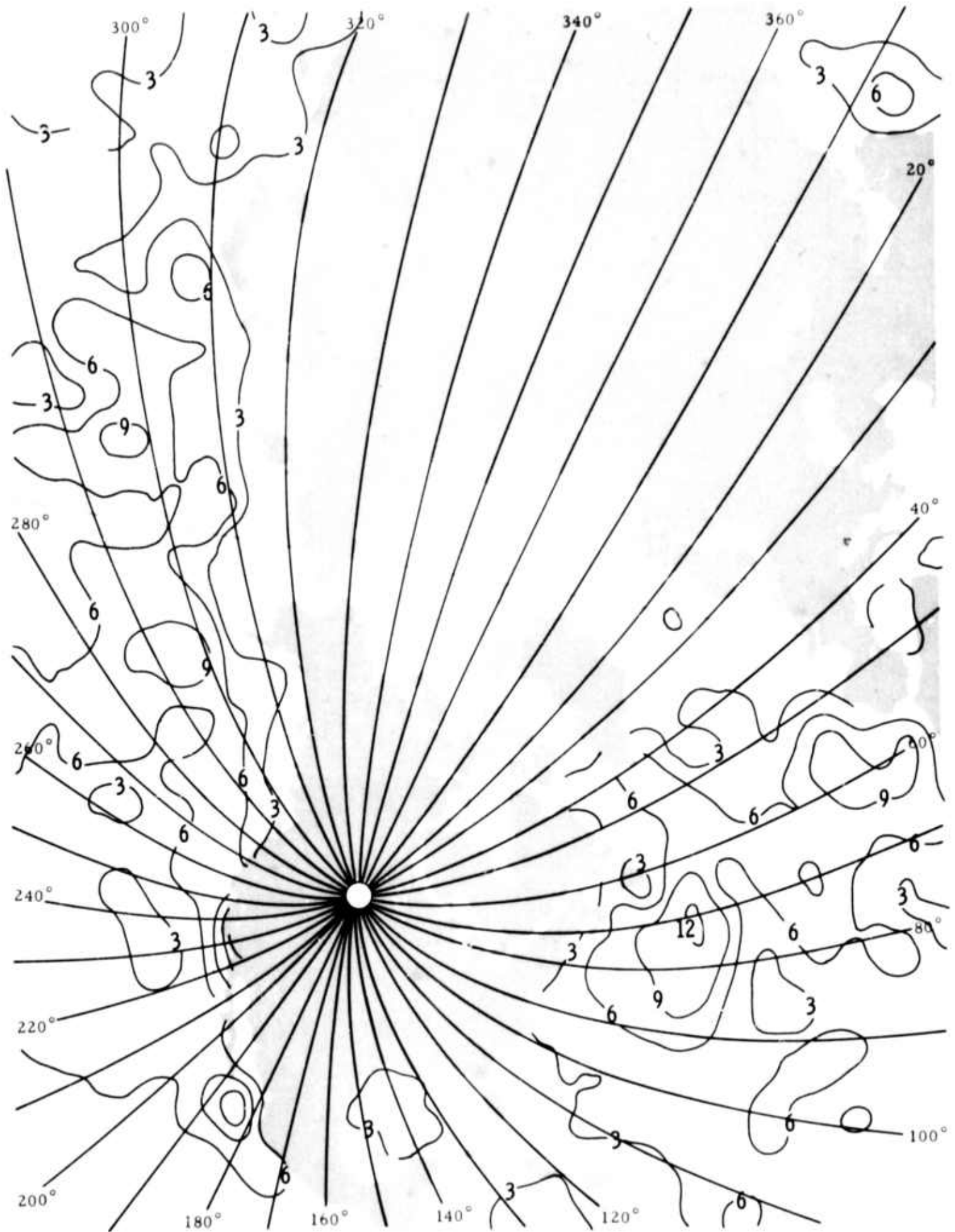
Figure III-24.   Waveheight Chart at 12.00 Hr, 11 May 1967
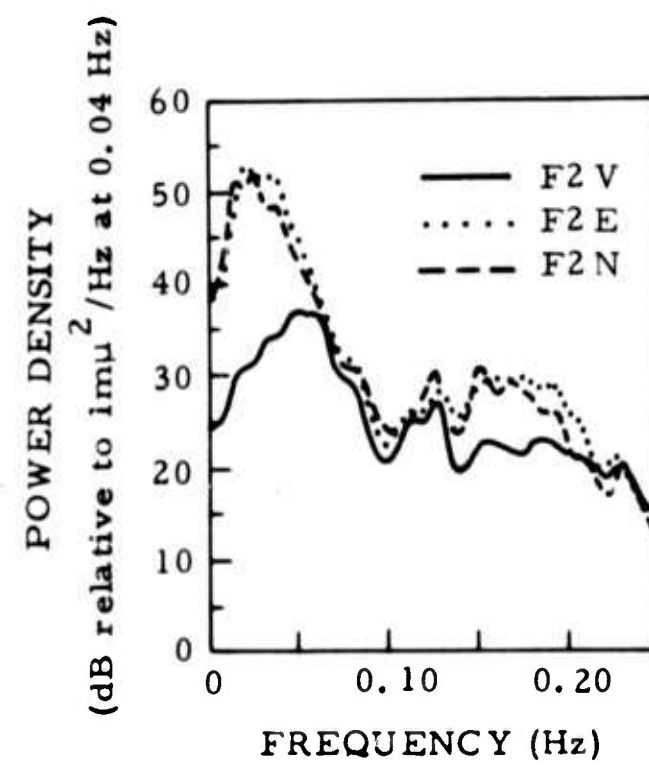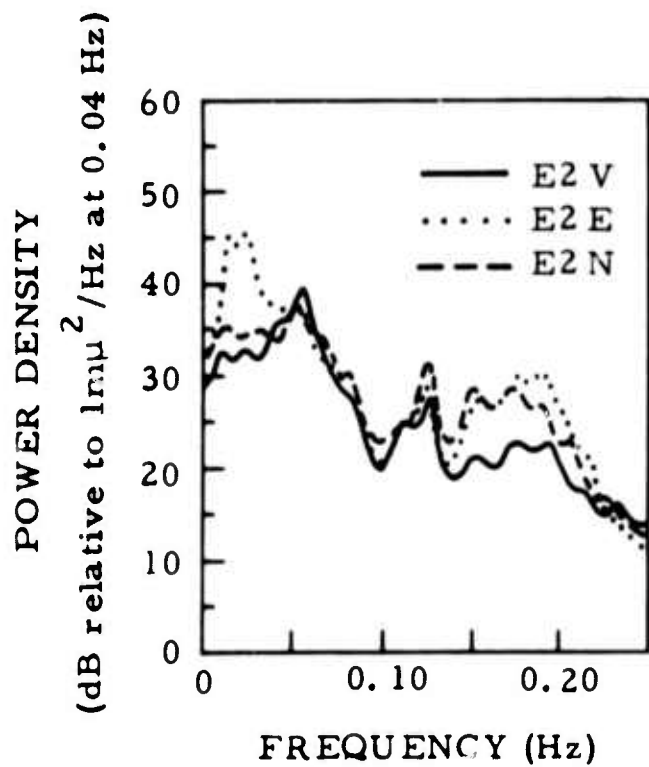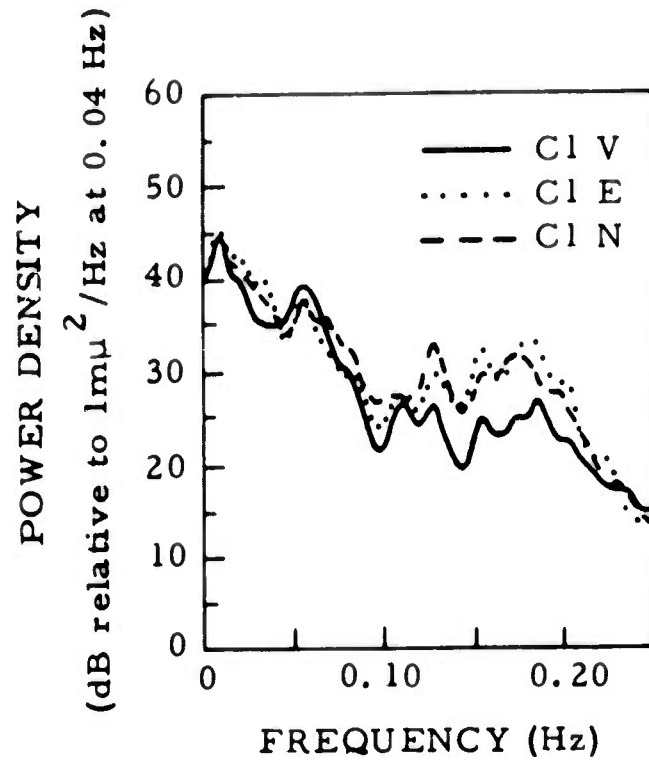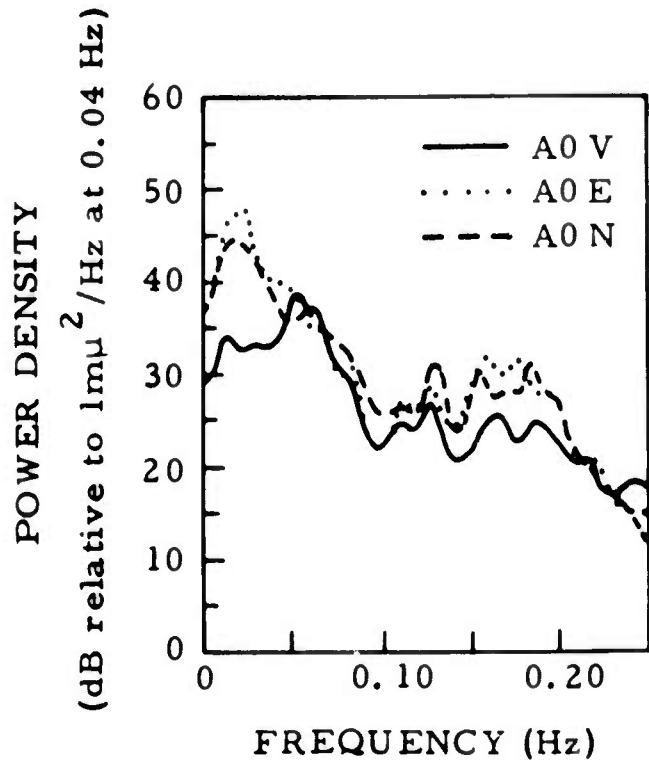
Figure III-25.   Power-Density Spectra of 11 May 1967 Noise

science services division
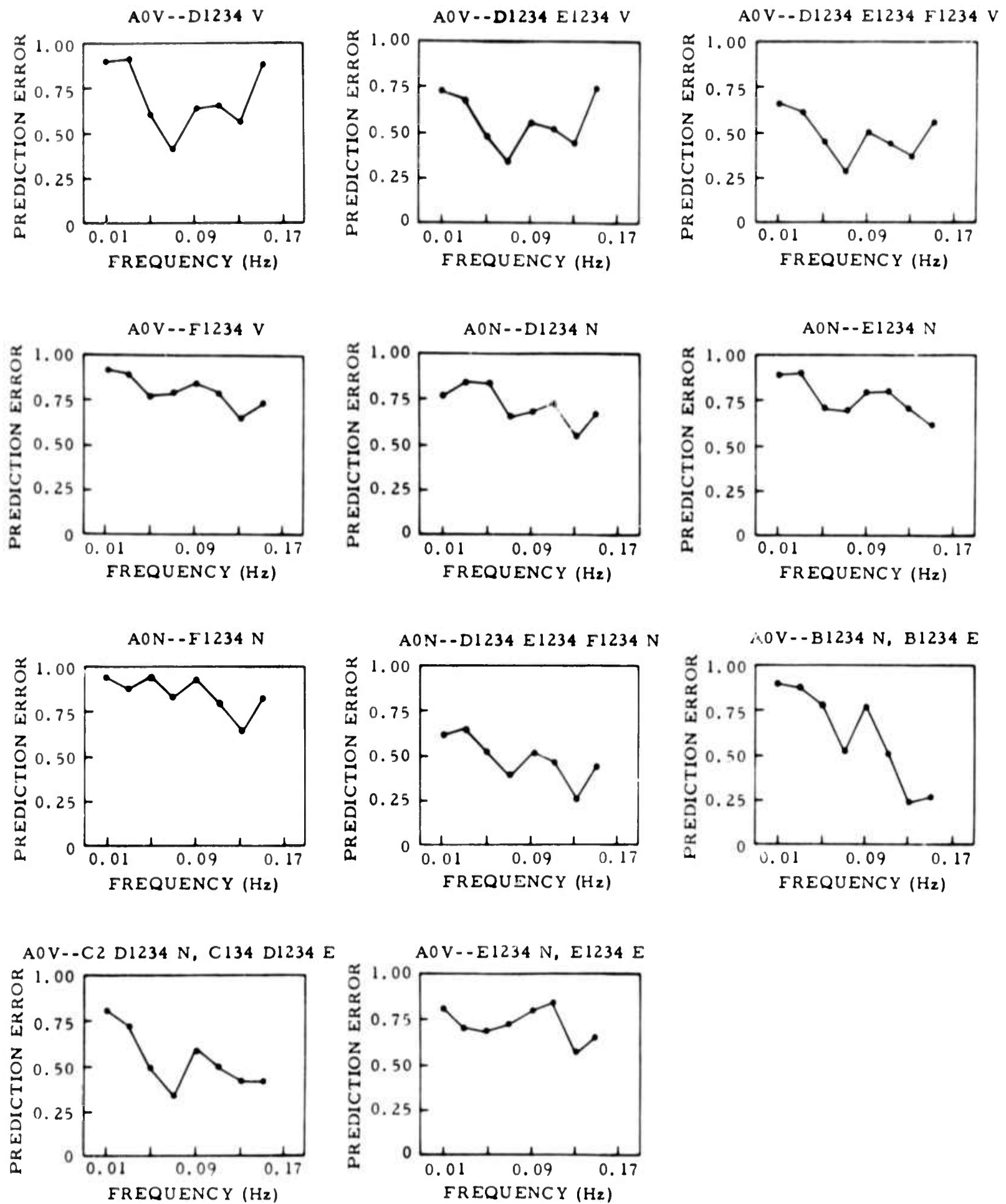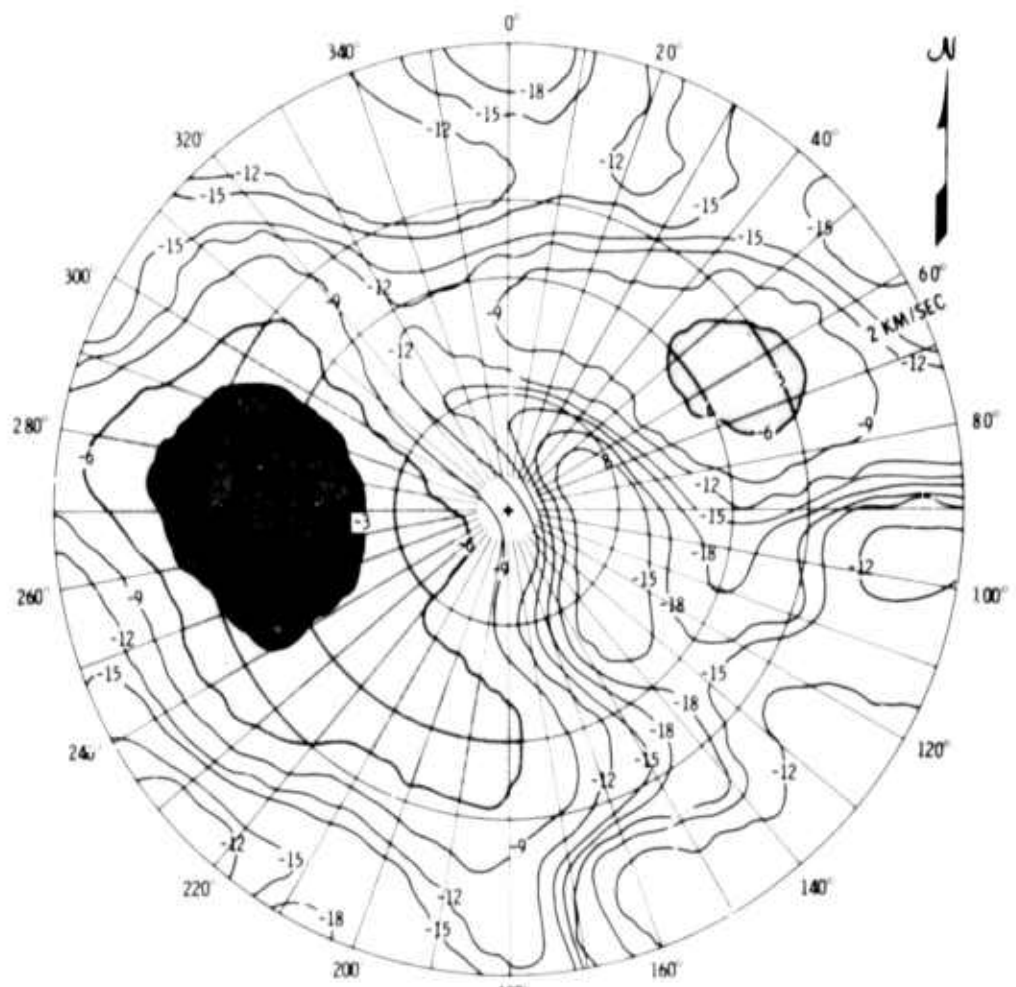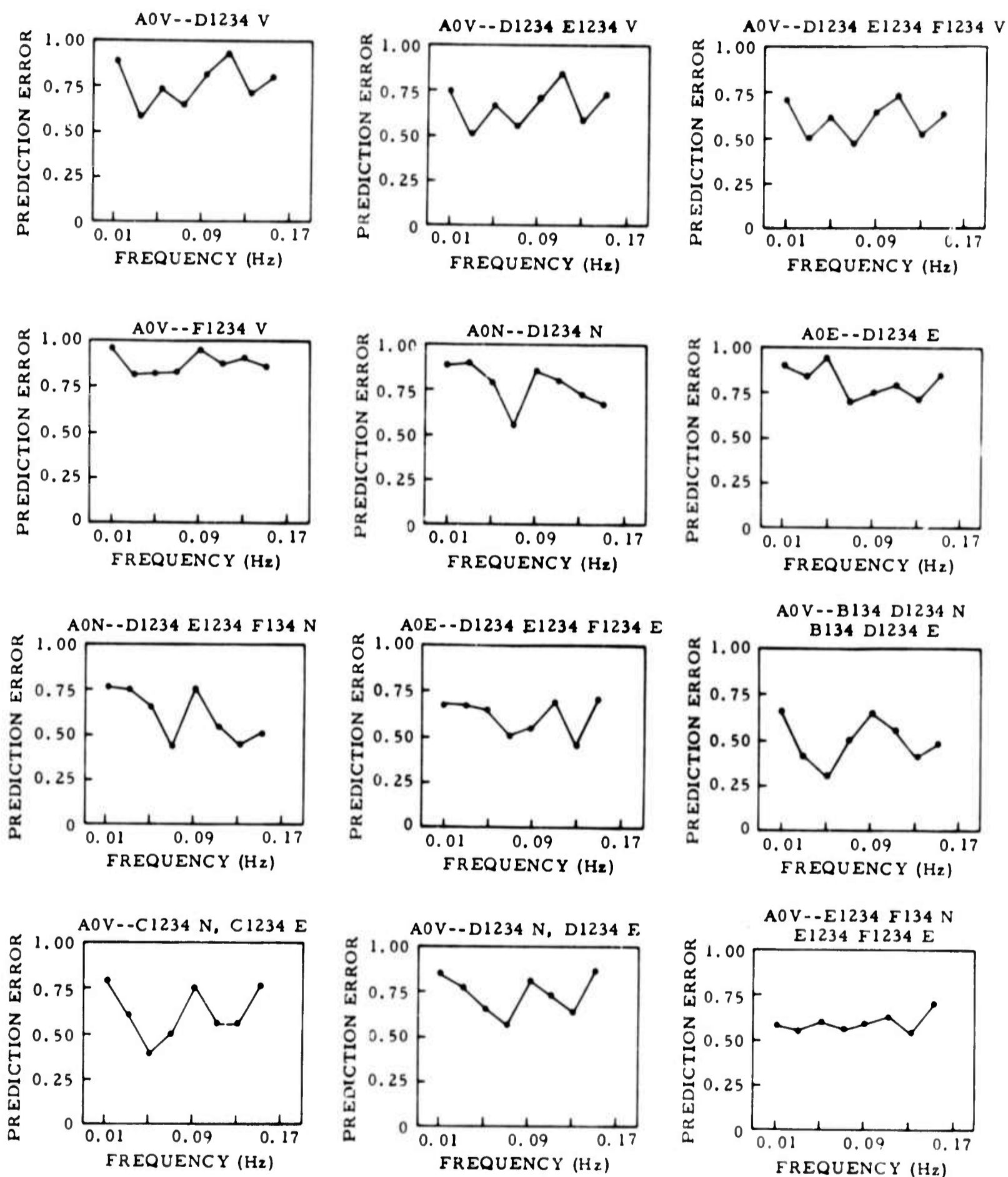
Figure III-26. Prediction-Error Plots for 11 May 1967 Noise Sample

VERTICAL
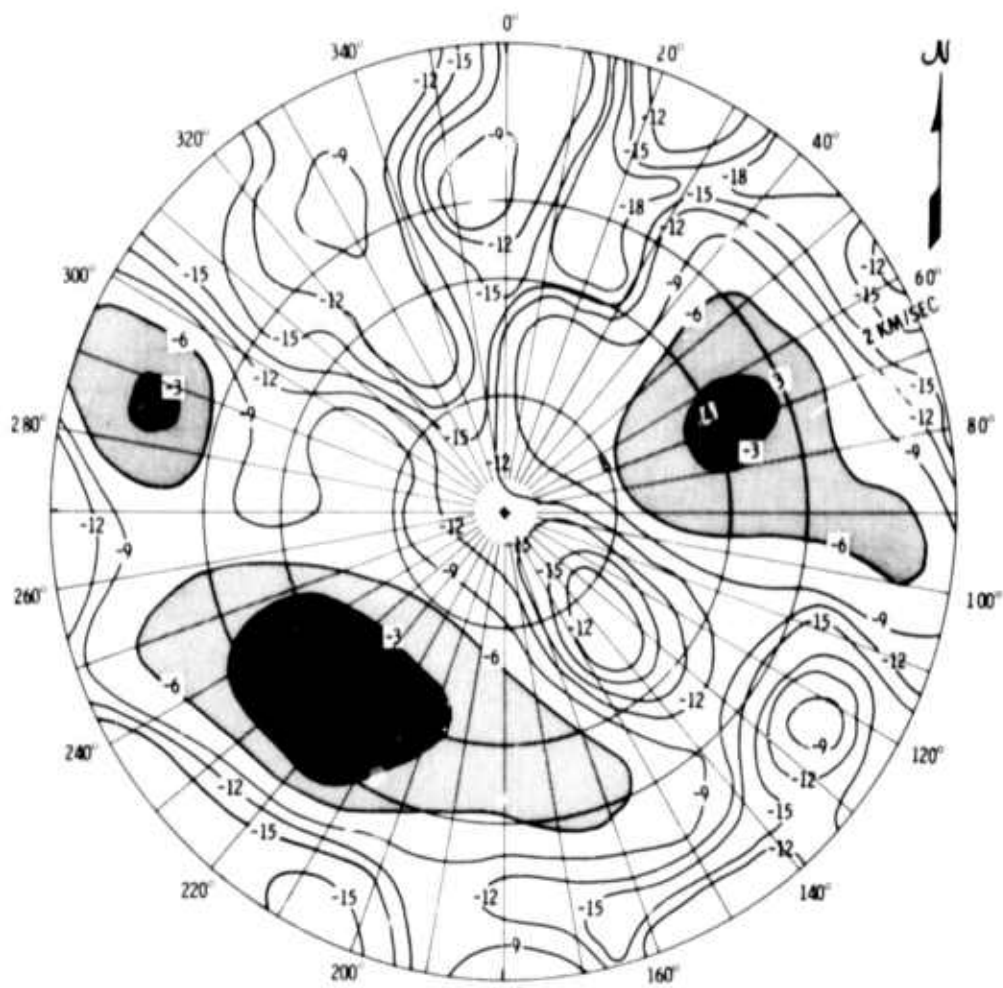
EAST-WEST
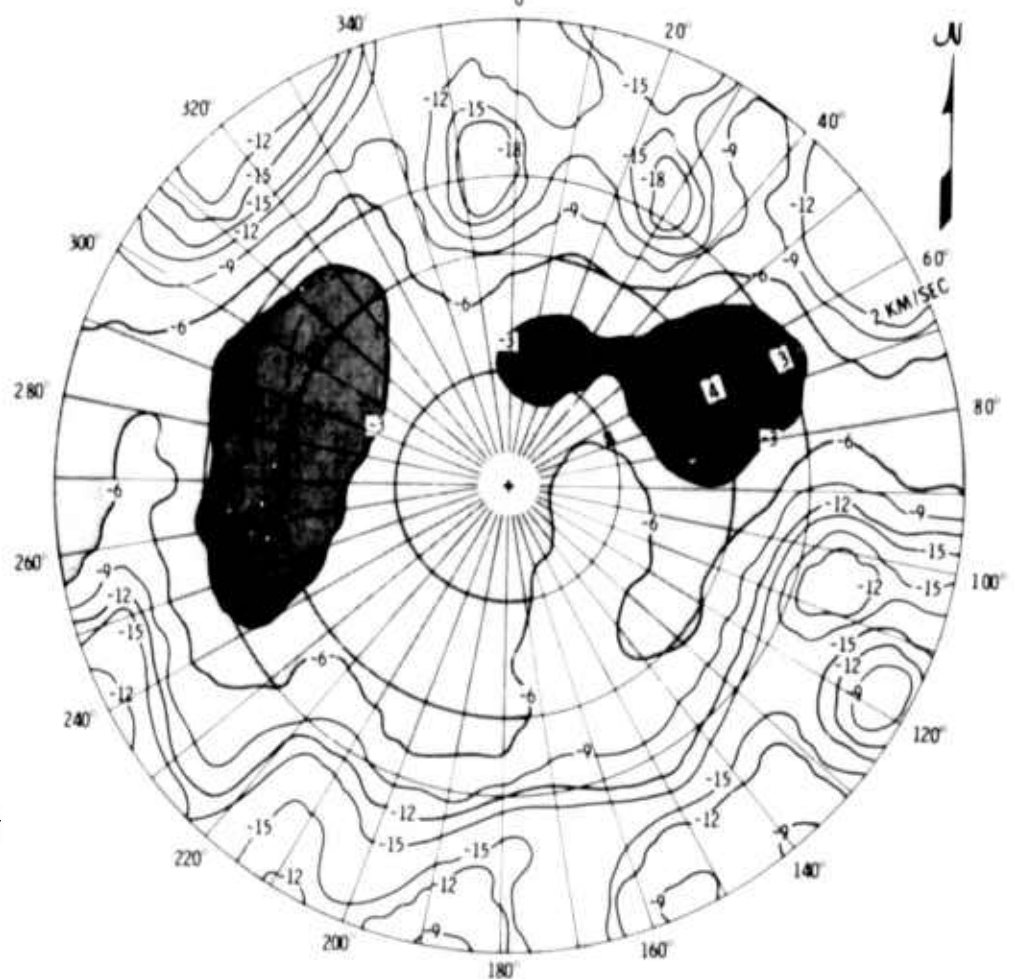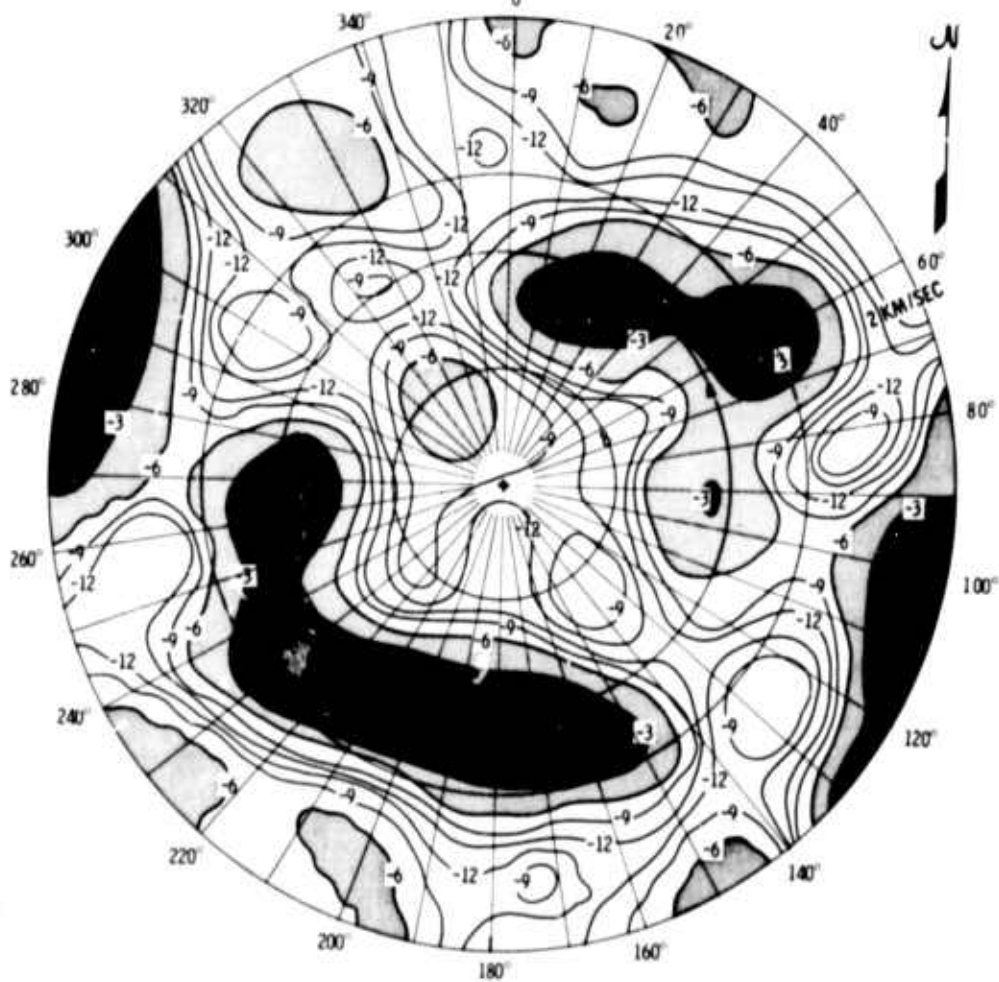
Figure III-27. Wavenumber Spectra at 0.06 Hz, 11 May 1967 Noise Sample
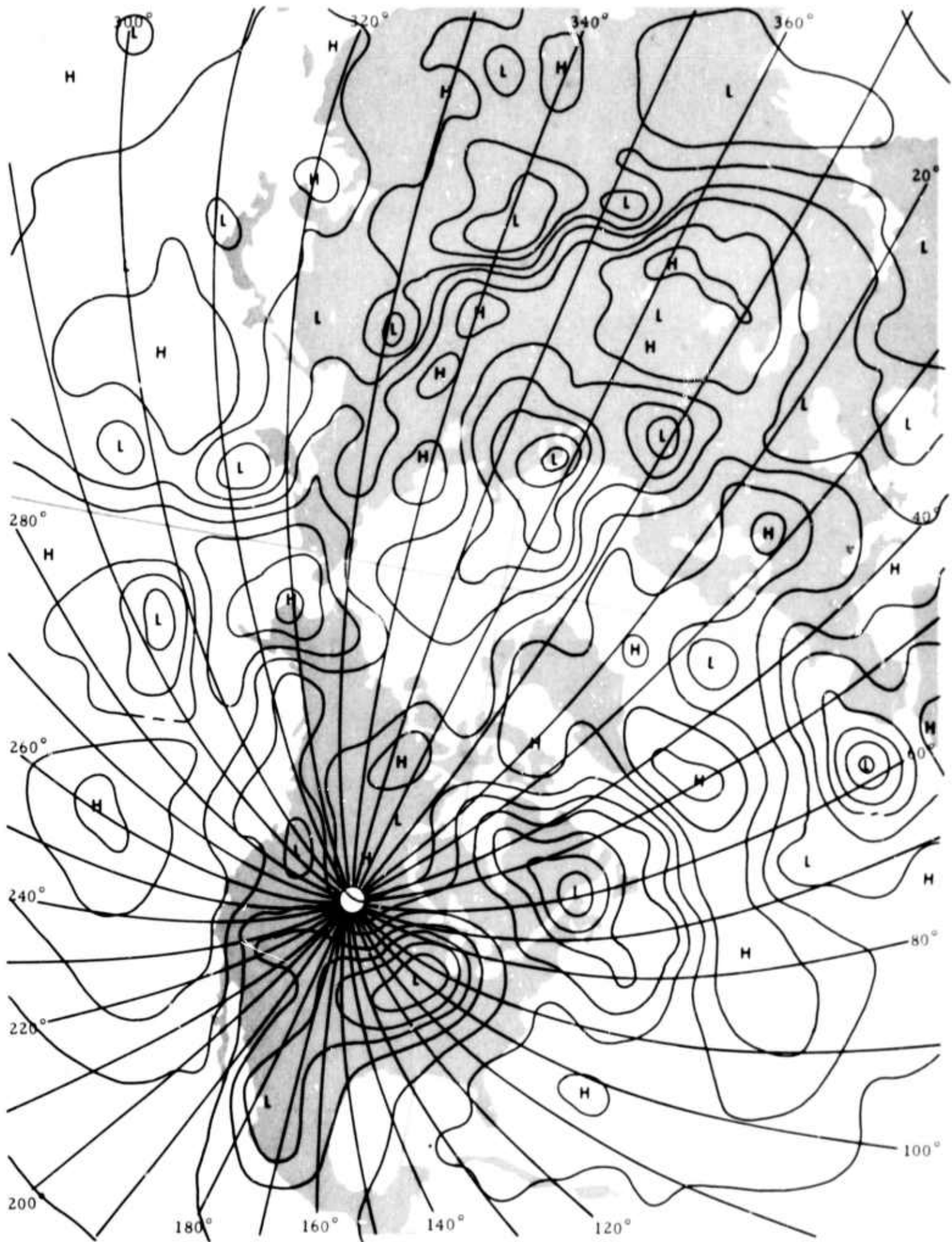
Figure III-28. Surface-Pressure Map at 06.00 Hr, 11 May 1967
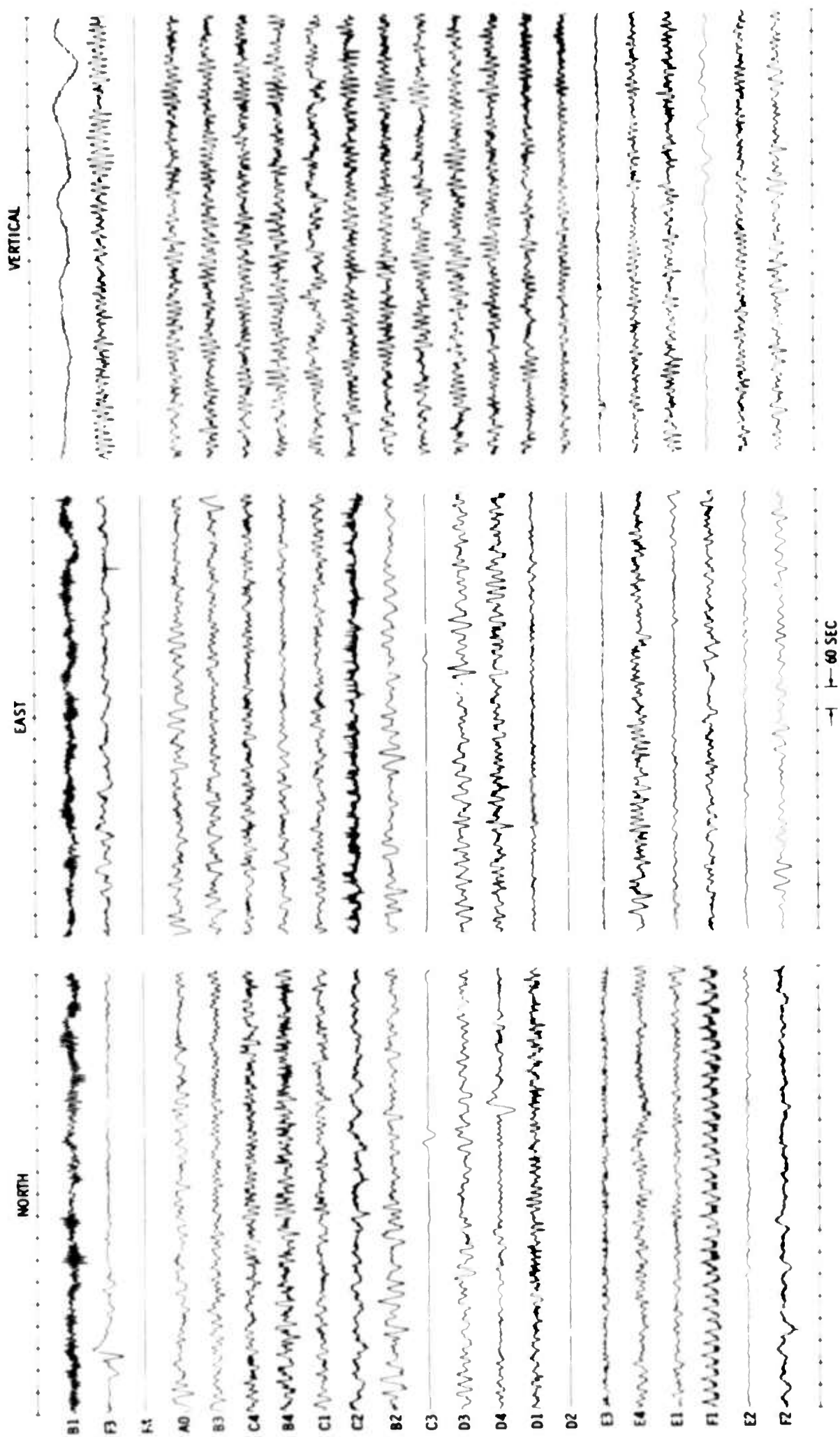
Figure III-29. 20-Min Segments of 10 July 1967 Noise Sample

VERTICAL

EAST

NORTH

60 SEC
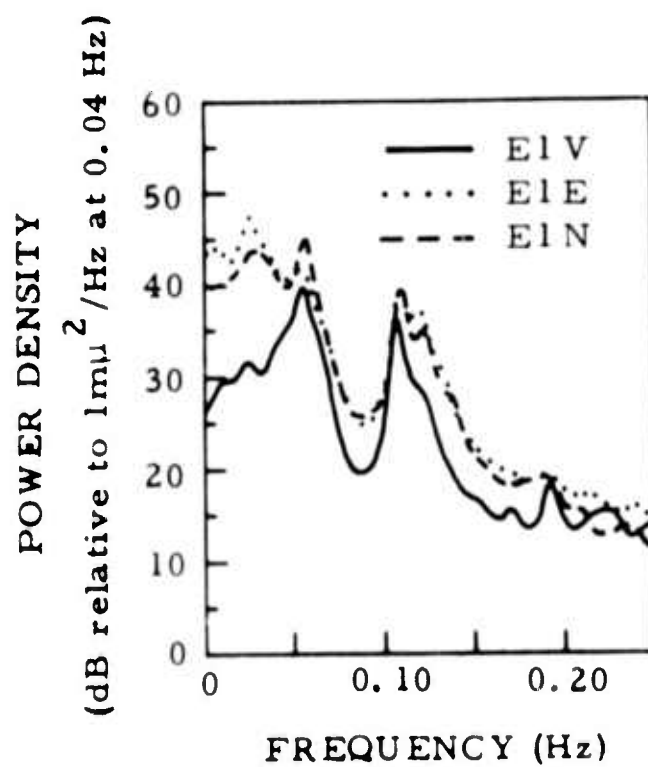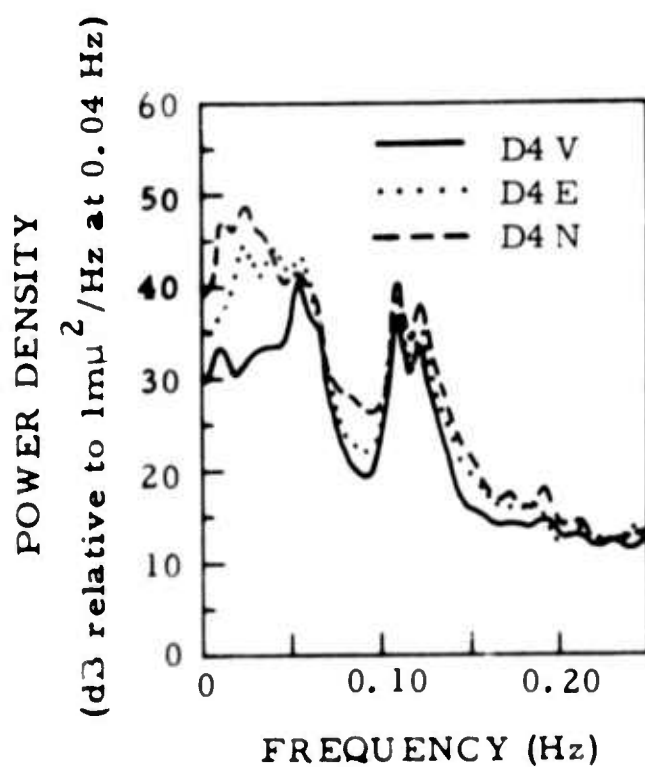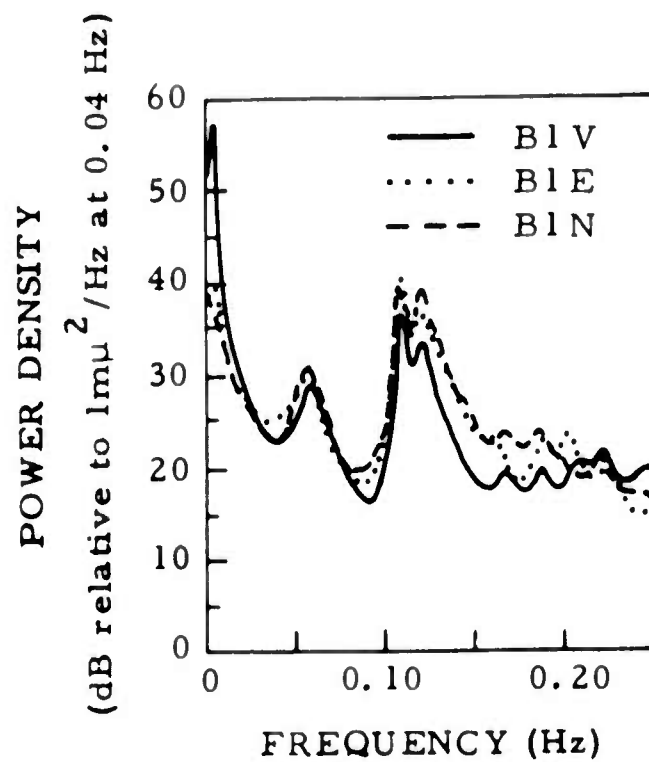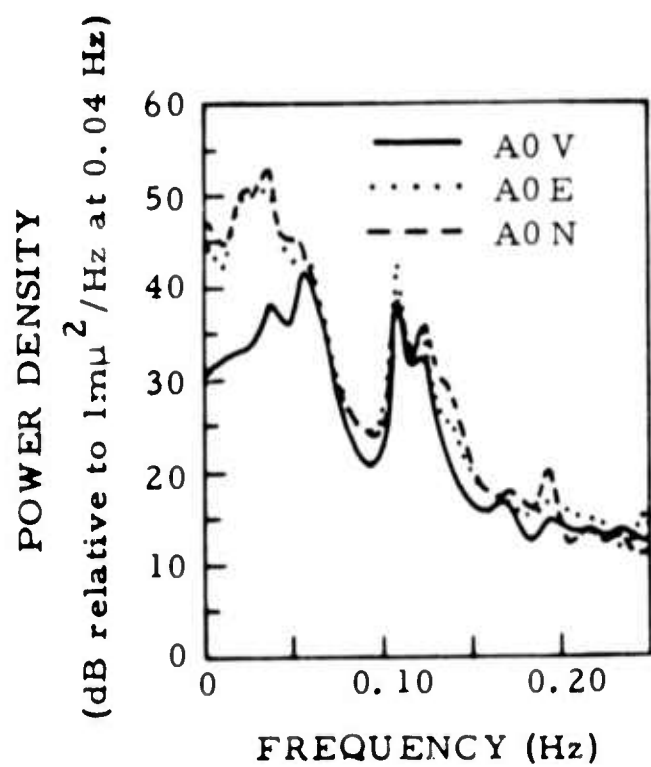
Figure III-30.   Power-Density Spectra of 10 July 1967 Noise
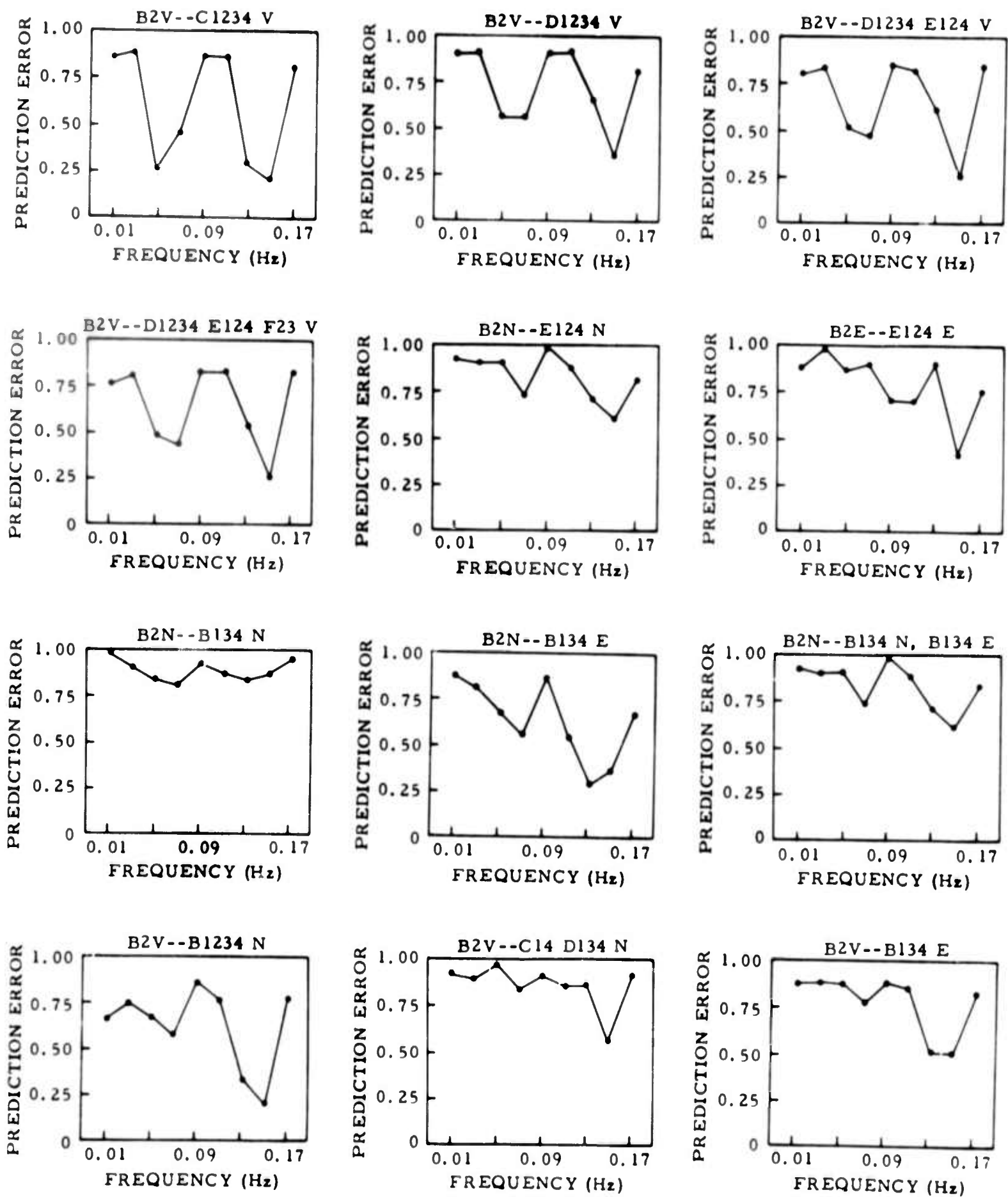
Figure III-31. Prediction-Error Plots for 10 July 1967 Noise Sample

science services division

VERTICAL
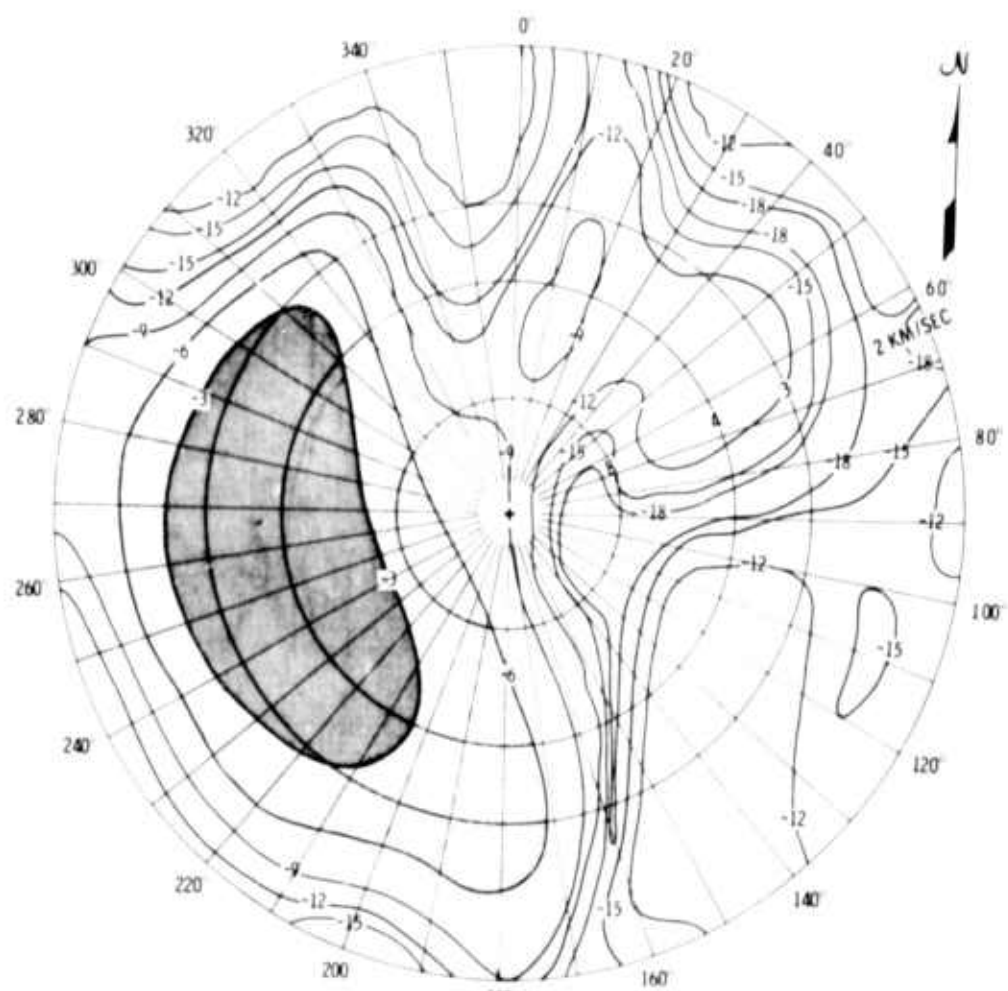
NORTH-SOUTH
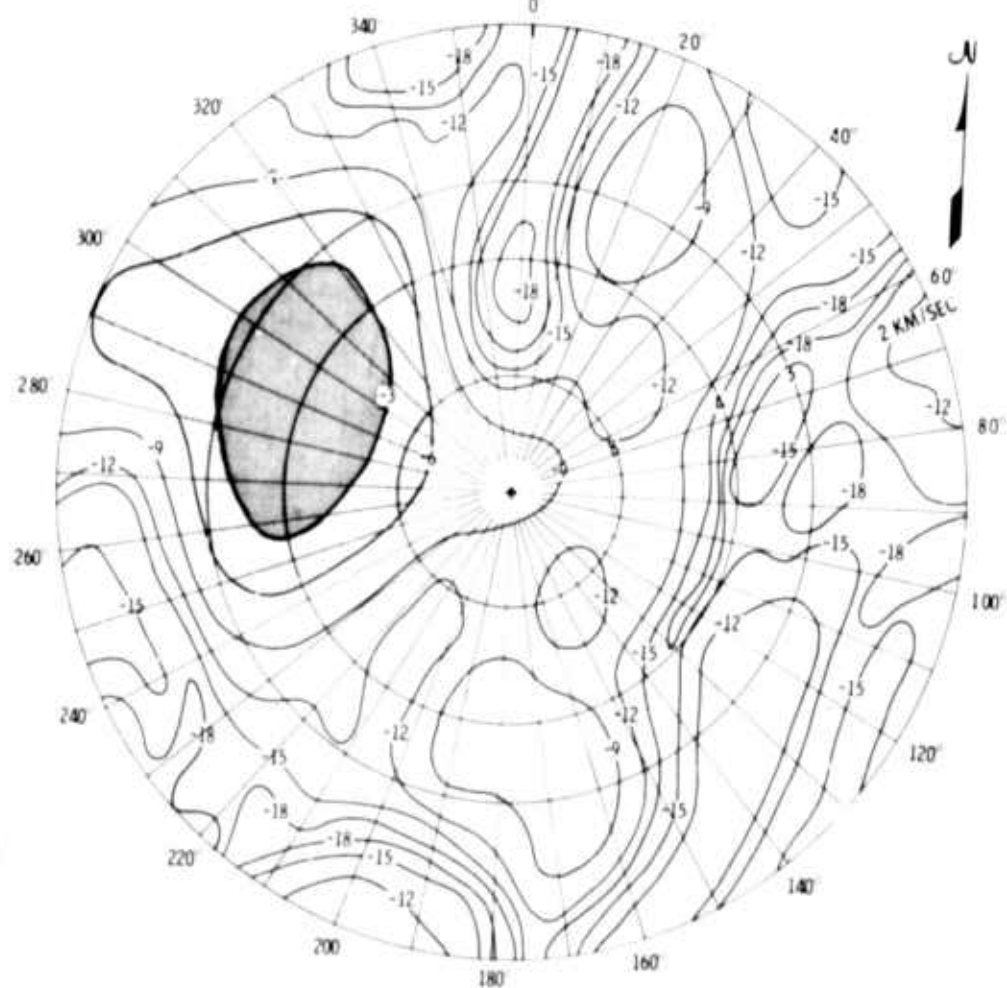
Figure III-32.   Wavenumber Spectra at 0.06 Hz, 10 July 1967 Noise Sample

science services division
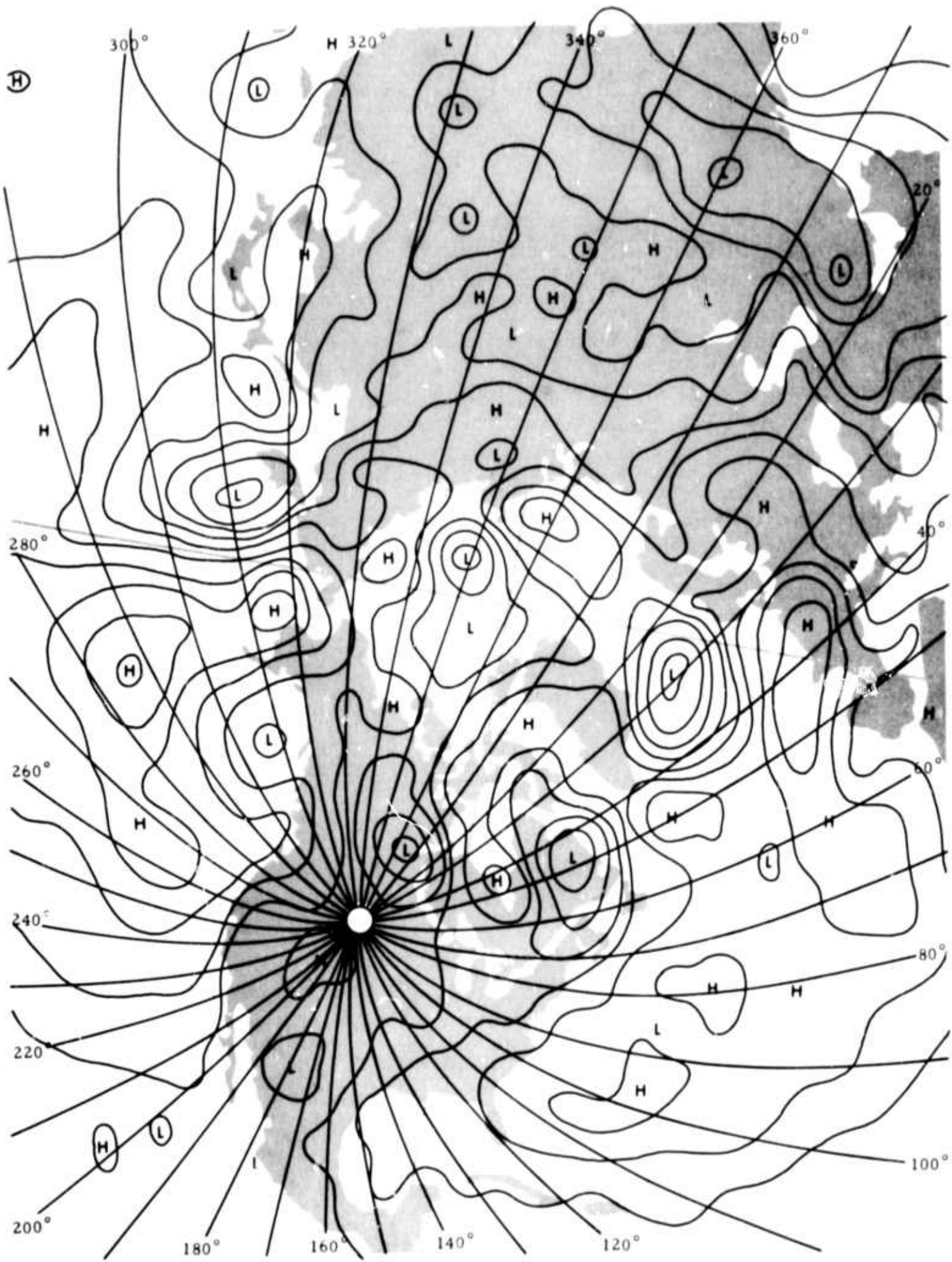
Figure III-33.   Surface-Pressure Map at 00.00 Hr, 10 July 1967

science services division
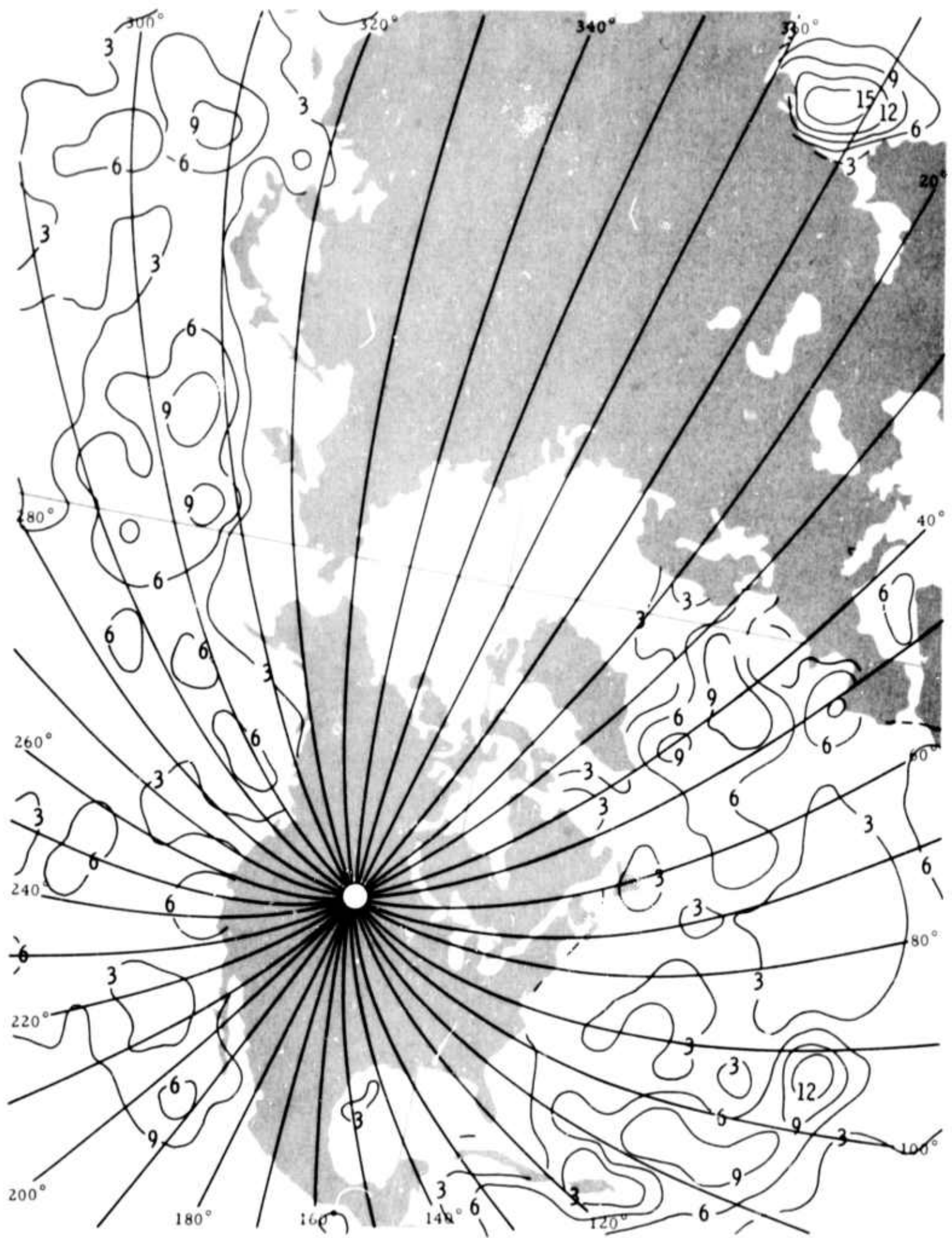
Figure III-34.   Waveheight Chart at 00.00 Hr, 10 July 1967
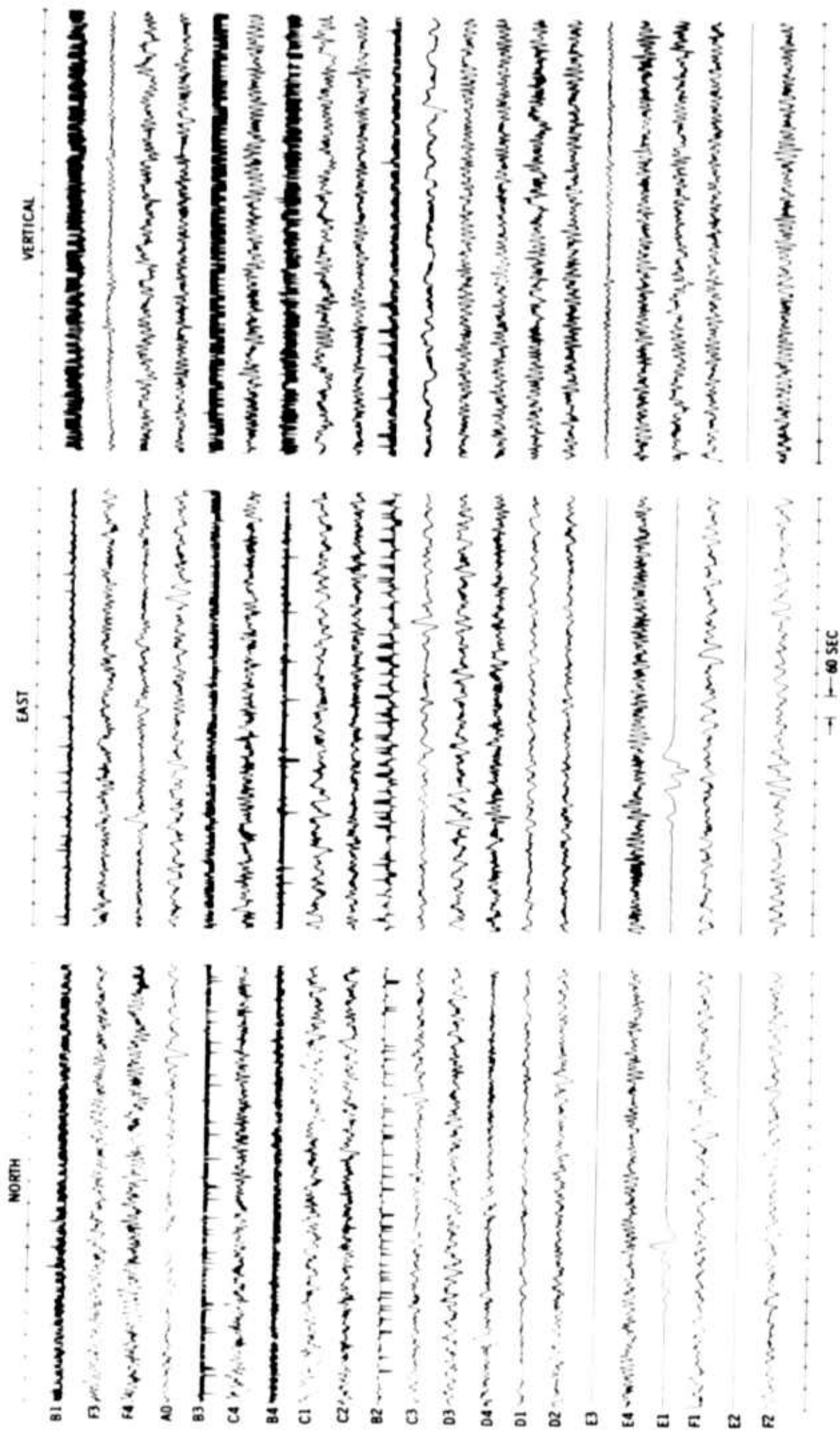
Figure III-35. 20-Min Segments of 7 October 1967 Noise Sample

science services division
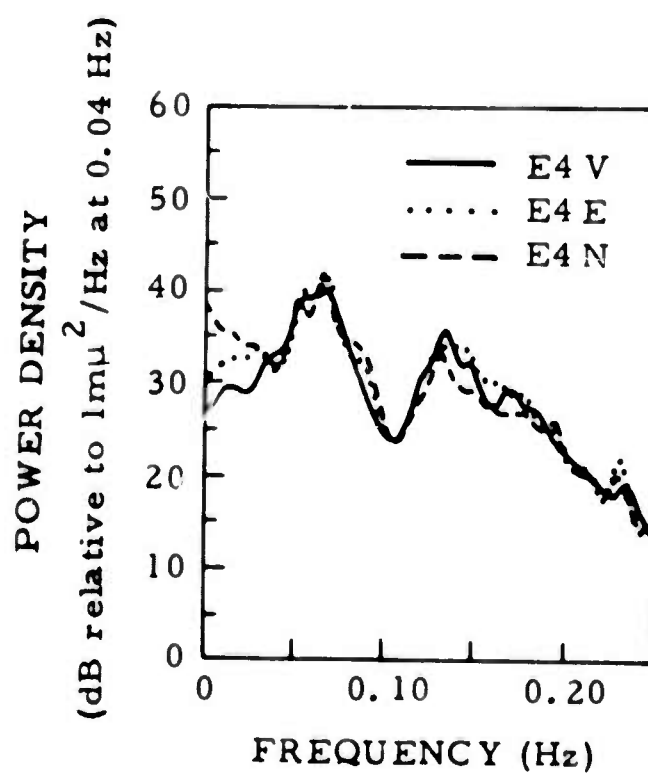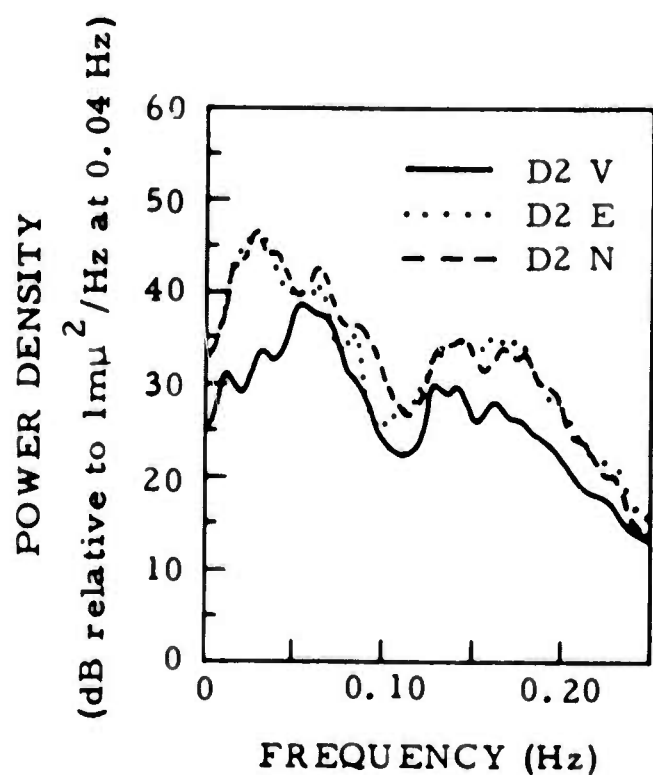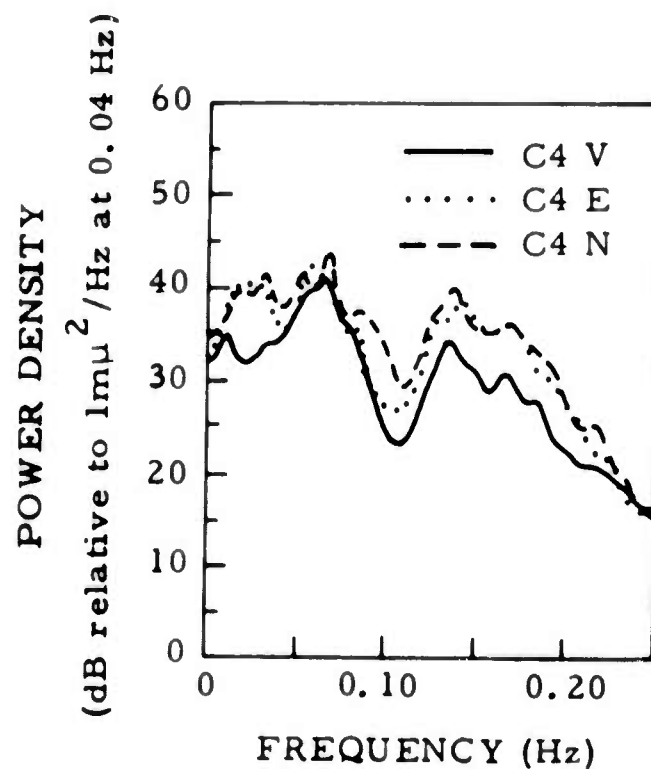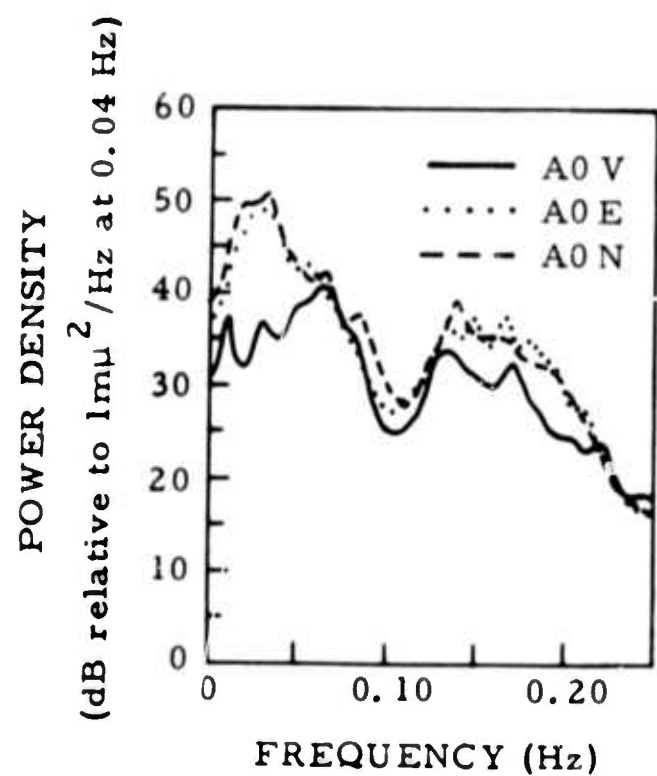
Figure III-36.   Power-Density Spectra of 7 October 1967 Noise

science services division
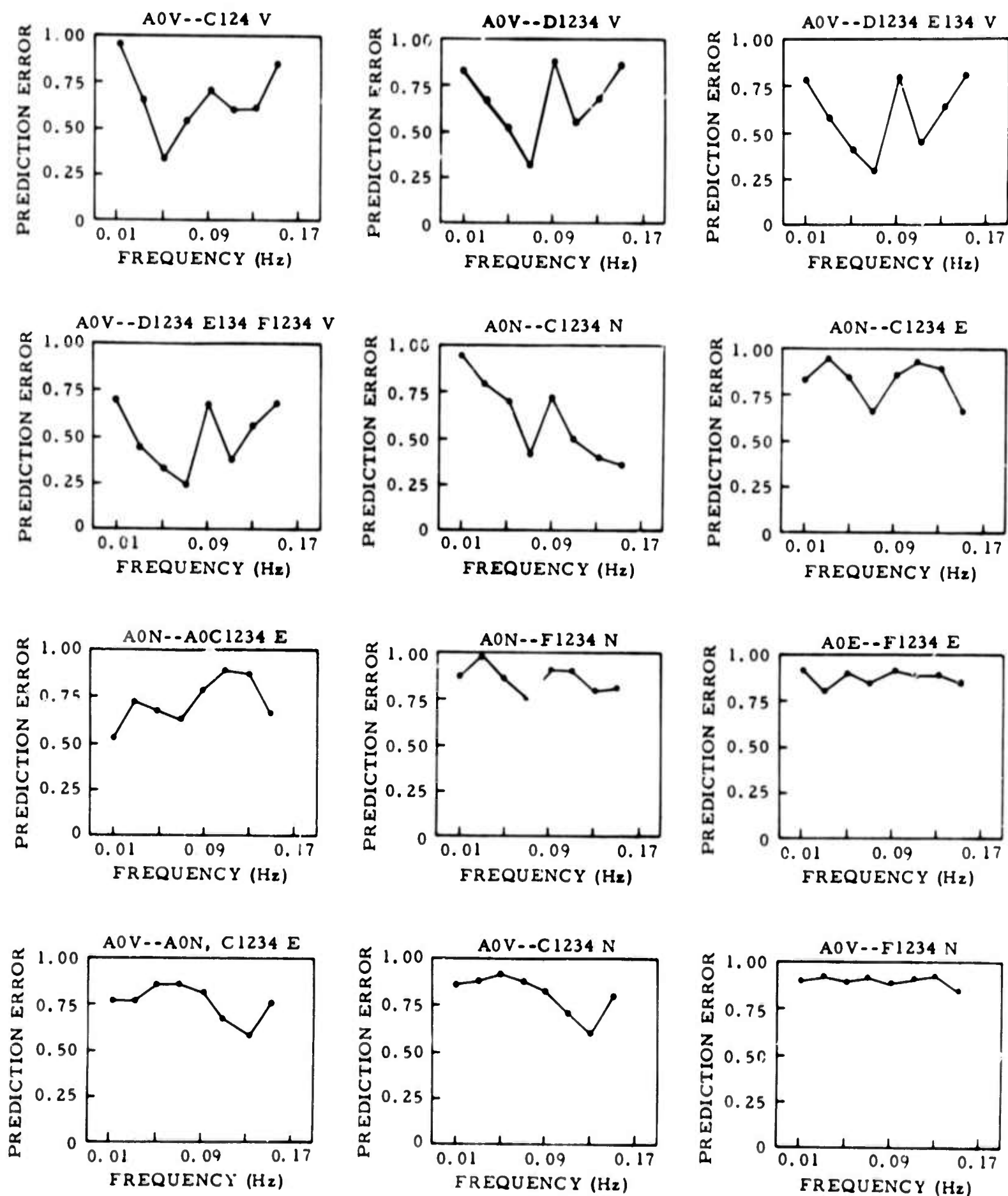
Figure III-37. Prediction-Error Plots for 7 October 1967 Noise Sample

science services division

VERTICAL
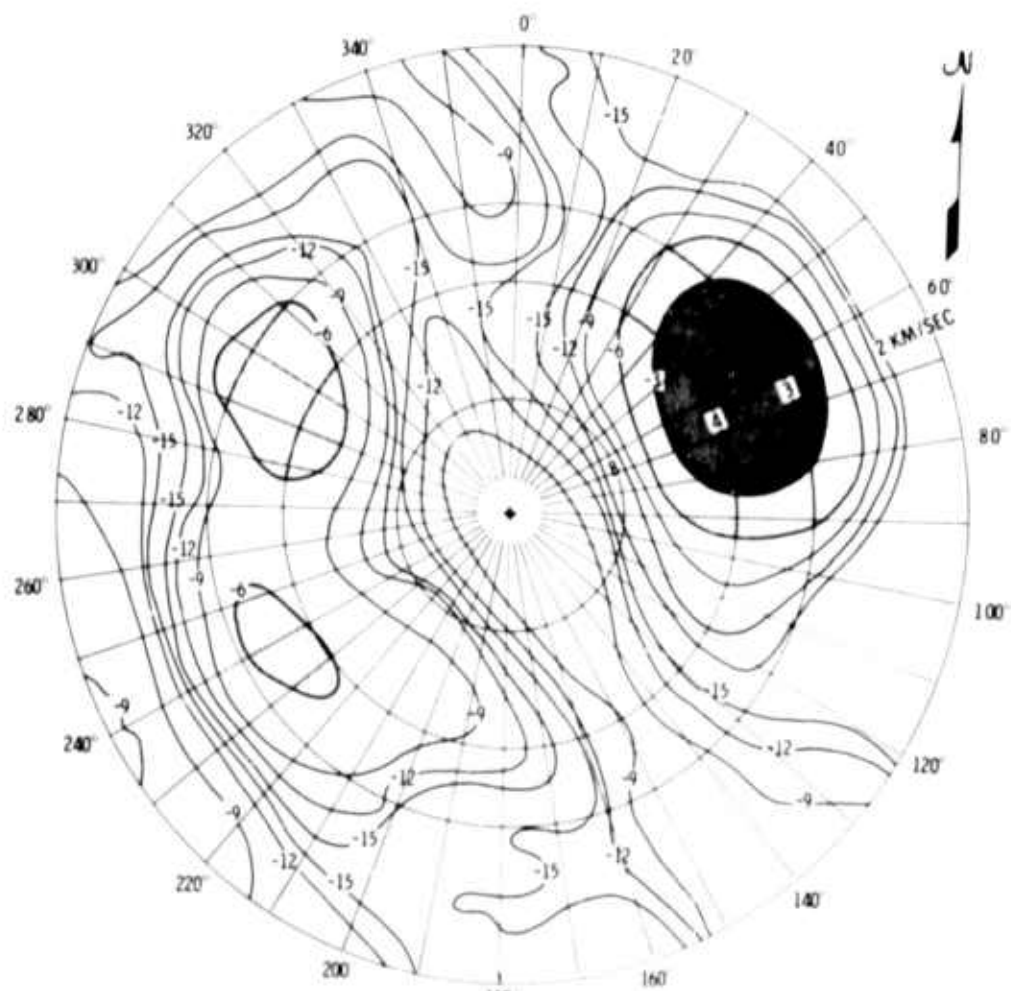
NORTH-SOUTH
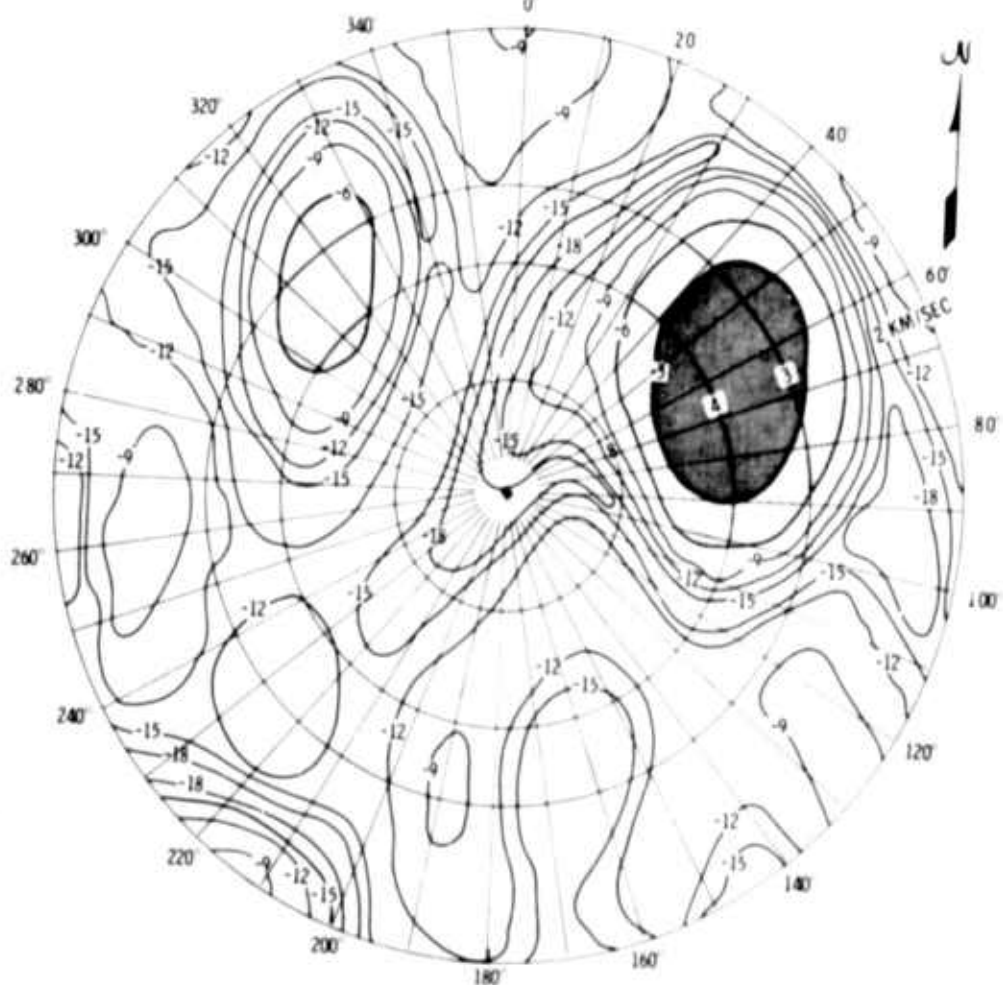
Figure III-38. Wavenumber Spectra at 0.06 Hz, 7 October 1967
Noise Sample

science services division
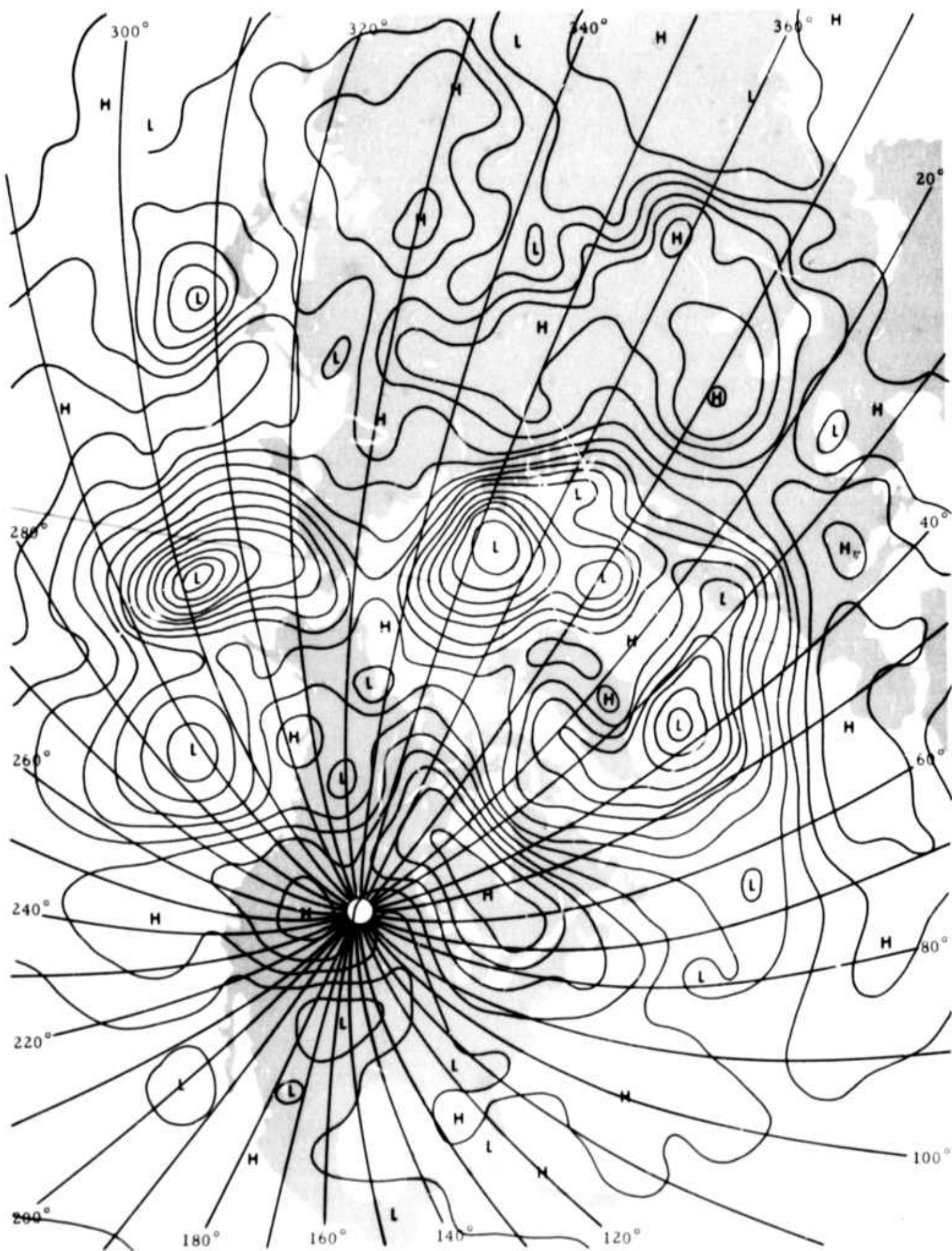
Figure III-39. Surface-Pressure Map at 12.00 Hr, 7 October 1967
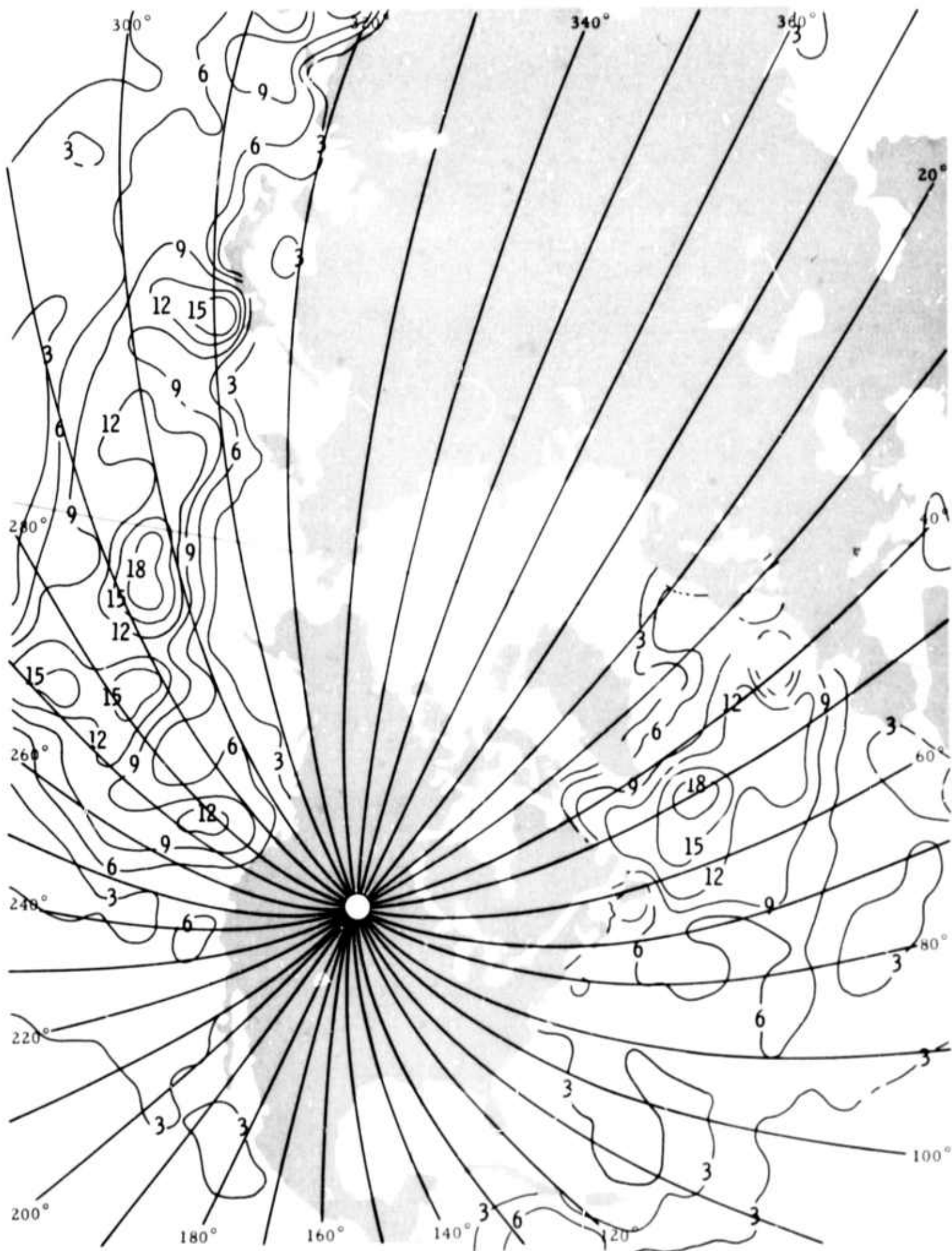
Figure III-40. Waveheight Chart at 12.00 Hr, 7 October 1967

SECTION IV

## COHERENCE BETWEEN MICROSEISMIC NOISE AND
MICROBAROGRAPHIC DATA

The results presented in this report and in several published papers, show that the noise below about 0.05 Hz is nonseismic.[4,5,6] Haubrich and MacKenzie suggest that wind action and changes in the atmospheric pressure may generate microseismic noise.[6] To investigate this, coherence between microseismic noise and microbarographic data was measured.

Five microbarographic instruments were in operation when the present samples were recorded. Their locations and characteristics are listed in Table IV-1. Two microbarographic instruments were at site A0. One instrument used different types of wind filters while the other used a single type of wind filter. The microbarograph sensor at site E was not used because it had very low sensitivity (Table IV-1).

Data containing microseismic noise consisted of the four segments from the 24 June long noise sample and the long noise sample from 10 July. Wiggly-trace monitors showed that only microbarographic data from the two A0 sensors were usable and both were very similar. All vertical data from seismic sensors were usable, but only 10 July horizontal data could be used.

Coherences and power-density spectra were computed using the technique described earlier. Auto- and crosspower spectra were smoothed over a 0.01 Hz (40 Δf) interval. Coherences between A0 vertical and microbarographic sensors were computed for all five samples, and all gave similar results. A typical prediction analysis plot is shown in Figure IV-1. Figure IV-2 shows the power spectra of the microbarographic data. In all cases,

the usable data had a power spectrum similar to the one pictured. Figure IV-3 shows the multiple coherence between the microbarograph and the horizontal traces at A0 for the 10 July noise sample.

Coherence between the air-pressure fluctuations and the long-period seismometer outputs is quite low but is statistically significant. Effects of air pressure upon the long-period instruments. if cause-and-effect-related, are related in some way more complicated than buoyancy only.

Table IV-1

MICROBAROGRAPH CHARACTERISTICS

Subarray	Location	3-db Response Period (sec)	Sensitivity (μbar) =14 v p-p	Type of Instruments
A0	Central Telemetry Housing	10 to 60	100	Pace-Hudson
A0	Central Telemetry Housing	10 to 60	100	Pace-Hudson
B1	LP Vault	10 to 80	98.3	Geotech
B4	LP Vault	10 to 80	87.3	Geotech
E3	LP Vault	10 to 600	1200	Pace-Hudson

Time-constant of wind filter was 10 sec in each case

science services division

A0V-A0 MICROBAROGRAPH

Figure IV-1. Prediction-Error Plot for A0 Vertical and Microbarograph Instruments, 24 June 1967 Noise Sample

A0 MICROBAROGRAPH--A0N, E
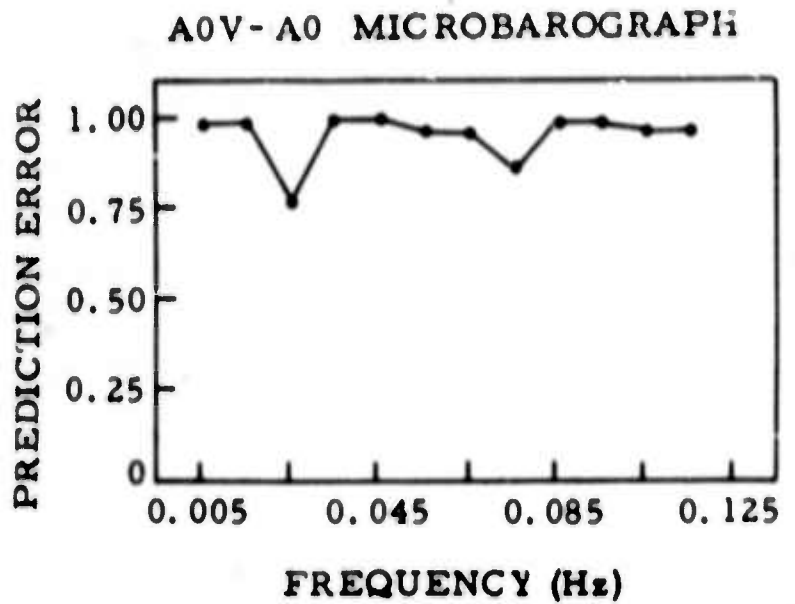
Figure IV-2. Prediction-Error Plot for A0 Microbarograph and Combinations of Horizontal Instruments, 10 July 1967 Noise Sample
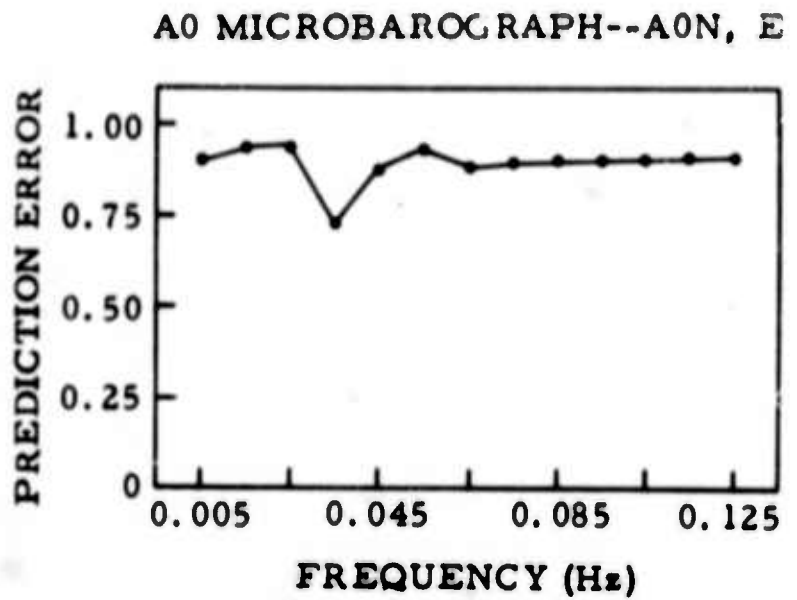
Figure IV-3. Power-Density Spectra of A0 Microbarographic Data, 24 June 1967 Noise
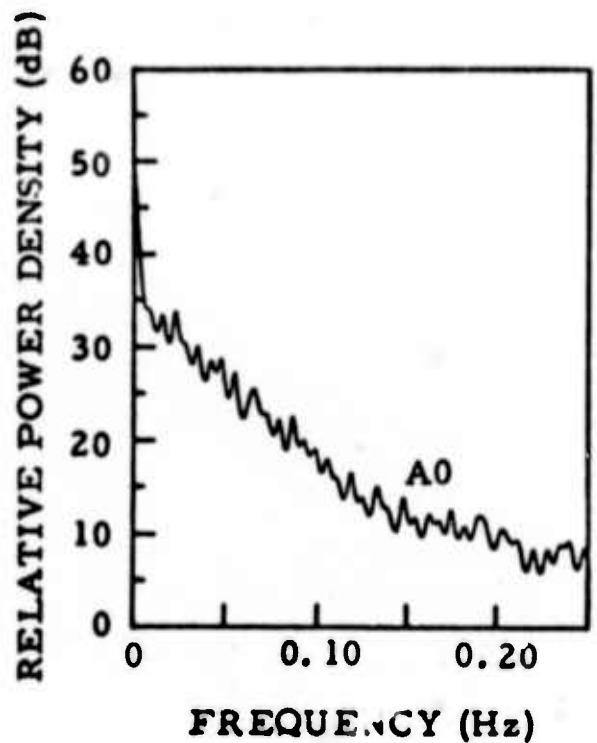
SECTION V

CONCLUSIONS

The summer noise samples are very similar to the quiet winter noise samples previously studied.[1] The following additional conclusions about long-period noise resulted from this study.

- Nonseismic noise below 0.05 Hz is not strongly correlated with a microbarograph at the same location (for both vertical and horizontal components). This lack of coherence appears to rule out a simple cause-and-effect relationship due to buoyancy.

- The 0.05- to 0.08-Hz microseism peak is dominated by fundamental Rayleigh-mode energy, even when this energy is reduced as much as possible by conditioning the vertical elements on knowing the horizontals. There was some indication of significant power density in the velocity P-wave region. The P-wave energy is at a very low level. In absence of strong storm activity, the 0.05- to 0.08-Hz noise peak probably tends toward isotropic fundamental Rayleigh-mode energy.

- On the most quiet data sample there is definite evidence of P-wave energy occurring in a very weak spectral peak near 0.13 Hz.

SECTION VI

REFERENCES

1. Texas Instruments Incorporated, 1967: Analysis of Long-Period Noise, Large-Array Signal and Noise Analysis, Spec. Rpt. 12, Contract AF 33(657)-16678, 8 Oct.

2. Burg, John P., 1967: Maximum Entropy Spectral Analysis, 37th Annual Meeting of Soc. of Exploration Geophysicists, Oklahoma City, Okla., Nov. (to be published).

3. Texas Instruments Incorporated, 1967: Short-Period Noise Coherences Among Subarrays, Large-Array Signal and Noise Analysis, Spec. Rpt. 13, Contract AF 33(657)-16678, 20 Oct.

4. Capon, J., 1968: Investigation of Long-Period Noise at LASA, Lincoln Lab. Tech. Note 1968-15, Contract AF 19(628)-5167, 3 Jun.

5. Toksöz, M.N., and R.T. Lacoss, 1968, Microseisms, mode structure and sources: Science, v. 159, n. 3817, p. 23, Feb.

6. Haubrich, R.A., and G.S. MacKenzie, Earth noise, 5 to 500 millicycles per second: J. of Geophys. Res., v. 70, n. 6., p. 1429-1440, 15 Mar.

DOCUMENT CONTROL DATA - R&D

(Security classification of title, body of abstract and indexing annotation must be entered when the overall report is classified)

1. ORIGINATING ACTIVITY (Corporate author)	2a. REPORT SECURITY CLASSIFICATION
Texas Instruments Incorporated Science Services Division P. O. Box 5621, Dallas, Texas 75222	Unclassified
	2b. GROUP

3. REPORT TITLE

ANALYSIS OF SUMMER LONG-PERIOD NOISE — LARGE-ARRAY SIGNAL AND NOISE ANALYSIS SPEC. RPT. NO. 24

4. DESCRIPTIVE NOTES (Type of report and inclusive dates)

Special Scientific

5. AUTHOR(S) (Last name, first name, initial)

Alam, Aftab

6. REPORT DATE	7a. TOTAL NO. OF PAGES	7b. NO. OF REFS
27 September 1968	57	6

8a. CONTRACT OR GRANT NO.	9a. ORIGINATOR'S REPORT NUMBER(S)
Contract AF 33(657)-16678	
b. PROJECT NO.	
VT/6707	
c.	9b. OTHER REPORT NO(S) (Any other numbers that may be assigned this report)
d.	

10. AVAILABILITY/LIMITATION NOTICES

This document is subject to special export controls and each transmittal to foreign governments or foreign nationals may be made only with prior approval of Chief, AFTAC.

11. SUPPLEMENTARY NOTES	12. SPONSORING MILITARY ACTIVITY
ARPA Order No. 599	Air Force Technical Applications Center VELA Seismological Center Headquarters, USAF, Washington, D.C.

13. ABSTRACT

The summer noise samples are very similar to the quiet winter noise samples. The following additional conclusions about long-period noise resulted from this study. Nonseismic noise below 0.05 Hz is not strongly correlated with a microbarograph at the same location (for both vertical and horizontal components). This lack of coherence appears to rule out a simple cause-and-effect relationship due to buoyancy. The 0.05- to 0.08-Hz microseism peak is dominated by fundamental Rayleigh-mode energy, even when this energy is reduced as much as possible by conditioning the vertical elements on knowing the horizontals. There was some indication of significant power density in the velocity P-wave region. The P-wave energy is at a very low level. In absence of strong storm activity, the 0.05- to 0.08-Hz noise peak probably tends toward isotropic fundamental Rayleigh-mode energy. On the most quiet data sample there is definite evidence of P-wave energy occurring in a very weak spectral peak near 0.13 Hz.

DD FORM 1473

KEY WORDS		LINK A		LINK B		LINK C	
		ROLE	WT	ROLE	WT	ROLE	WT
Large-Array Signal and Noise Analysis							
LASA							
Summer Long-Period Noise							
Microbarographic Correlation							

INSTRUCTIONS

1. **ORIGINATING ACTIVITY:** Enter the name and address of the contractor, subcontractor, grantee, Department of Defense activity or other organization (corporate author) issuing the report.

2a. **REPORT SECURITY CLASSIFICATION:** Enter the overall security classification of the report. Indicate whether "Restricted Data" is included. Marking is to be in accordance with appropriate security regulations.

2b. **GROUP:** Automatic downgrading is specified in DoD Directive 5200.10 and Armed Forces Industrial Manual. Enter the group number. Also, when applicable, show that optional markings have been used for Group 3 and Group 4 as authorized.

3. **REPORT TITLE:** Enter the complete report title in all capital letters. Titles in all cases should be unclassified. If a meaningful title cannot be selected without classification, show title classification in all capitals in parenthesis immediately following the title.

4. **DESCRIPTIVE NOTES:** If appropriate, enter the type of report, e.g., interim, progress, summary, annual, or final. Give the inclusive dates when a specific reporting period is covered.

5. **AUTHOR(S):** Enter the name(s) of author(s) as shown on or in the report. Enter last name, first name, middle initial. If military, show rank and branch of service. The name of the principal author is an absolute minimum requirement.

6. **REPORT DATE:** Enter the date of the report as day, month, year; or month, year. If more than one date appears on the report, use date of publication.

7a. **TOTAL NUMBER OF PAGES:** The total page count should follow normal pagination procedures, i.e., enter the number of pages containing information.

7b. **NUMBER OF REFERENCES:** Enter the total number of references cited in the report.

8a. **CONTRACT OR GRANT NUMBER:** If appropriate, enter the applicable number of the contract or grant under which the report was written.

8b, 8c, & 8d. **PROJECT NUMBER:** Enter the appropriate military department identification, such as project number, subproject number, system numbers, task number, etc.

9a. **ORIGINATOR'S REPORT NUMBER(S):** Enter the official report number by which the document will be identified and controlled by the originating activity. This number must be unique to this report.

9b. **OTHER REPORT NUMBER(S):** If the report has been assigned any other report numbers (either by the originator or by the sponsor), also enter this number(s).

10. **AVAILABILITY/LIMITATION NOTICES:** Enter any limitations on further dissemination of the report, other than those imposed by security classification, using standard statements such as:

(1) "Qualified requesters may obtain copies of this report from DDC."

(2) "Foreign announcement and dissemination of this report by DDC is not authorized."

(3) "U. S. Government agencies may obtain copies of this report directly from DDC. Other qualified DDC users shall request through

_____."

(4) "U. S. military agencies may obtain copies of this report directly from DDC. Other qualified users shall request through

_____."

(5) "All distribution of this report is controlled. Qualified DDC users shall request through

_____."

If the report has been furnished to the Office of Technical Services, Department of Commerce, for sale to the public, indicate this fact and enter the price, if known.

11. **SUPPLEMENTARY NOTES:** Use for additional explanatory notes.

12. **SPONSORING MILITARY ACTIVITY:** Enter the name of the departmental project office or laboratory sponsoring (paying for) the research and development. Include address.

13. **ABSTRACT:** Enter an abstract giving a brief and factual summary of the document indicative of the report, even though it may also appear elsewhere in the body of the technical report. If additional space is required, a continuation sheet shall be attached.

It is highly desirable that the abstract of classified reports be unclassified. Each paragraph of the abstract shall end with an indication of the military security classification of the information in the paragraph, represented as (TS), (S), (C), or (U).

There is no limitation on the length of the abstract. However, the suggested length is from 150 to 225 words.

14. **KEY WORDS:** Key words are technically meaningful terms or short phrases that characterize a report and may be used as index entries for cataloging the report. Key words must be selected so that no security classification is required. Identifiers, such as equipment model designation, trade name, military project code name, geographic location, may be used as key words but will be followed by an indication of technical context. The assignment of links, rules, and weights is optional.

GPO 886-551